© 2015. Published by The Company of Biologists Ltd | Development (2015) 142, 3537-3548 doi:10.1242/dev.126144

RESEARCH ARTICLE

ABCC5 is required for cAMP-mediated hindgut invagination in sea urchin embryos

Lauren E. Shipp*, Rose Z. Hill‡, Gary W. Moy, Tufan Gökırmak and Amro Hamdoun§

ABSTRACT

ATP-binding cassette (ABC) transporters are evolutionarily conserved proteins that pump diverse substrates across membranes. Many are known to efflux signaling molecules and are extensively expressed during development. However, the role of transporters in moving extracellular signals that regulate embryogenesis is largely unexplored. Here, we show that a mesodermal ABCC (MRP) transporter is necessary for endodermal gut morphogenesis in sea urchin embryos. This transporter, *Sp*-ABCC5a (C5a), is expressed in pigment cells and their precursors, which are a subset of the non-skeletogenic mesoderm (NSM) cells. *C5a* expression depends on Delta/Notch signaling from skeletogenic mesoderm and is downstream of Gcm in the aboral NSM gene regulatory network. Long-term imaging of development reveals that C5a knockdown embryos gastrulate, but ~90% develop a prolapse of the hindgut by the late prism stage (~8 h after C5a protein expression normally peaks). Since C5a orthologs efflux cyclic nucleotides, and cAMP-dependent protein kinase (*Sp*-CAPK/PKA) is expressed in pigment cells, we examined whether C5a could be involved in gastrulation through cAMP transport. Consistent with this hypothesis, membrane-permeable pCPT-cAMP rescues the prolapse phenotype in C5a knockdown embryos, and causes archenteron hyper-invagination in control embryos. In addition, the cAMP-producing enzyme soluble adenylyl cyclase (sAC) is expressed in pigment cells, and its inhibition impairs gastrulation. Together, our data support a model in which C5a transports sAC-derived cAMP from pigment cells to control late invagination of the hindgut. Little is known about the ancestral functions of ABCC5/MRP5 transporters, and this study reveals a novel role for these proteins in mesoderm-endoderm signaling during embryogenesis.

KEY WORDS: ABC transporter, ABCC5, MRP5, cAMP, Developmental signaling, Gastrulation, Soluble adenylyl cyclase (sAC), Sea urchin

INTRODUCTION

Morphogenesis is choreographed by extracellular signals. These include short-range signals between neighboring cells, and long-range signals that work across the embryo. A central question is how long-range signals are distributed to act specifically. Active transport is an essential mechanism for secretion and organization of molecules that act over long distances (Müller and Schier, 2011). For instance, in plant root development, precise spatial and temporal distribution of transporters establishes directional gradients that direct tip growth (Robert and Friml, 2009), and in fly development active transporters secrete molecules that attract germ cells (Ricardo and Lehmann, 2009). Despite this importance of active signaling in development, transporters are largely unexplored in animal embryos. Tackling their biology is important, because it could help define the origin and destination of secreted signals.

Here, we report a novel developmental signaling function of a member of the ATP-binding cassette (ABC) transporter family. This family includes active transporters that translocate signaling molecules across membranes. ABC transporters are found in all organisms and have a wide range of endogenous and exogenous substrates. Among the ABC family are the multifunctional 'multidrug resistance' (MDR) transporters of the ABCB, -C, and -G subfamilies, which have primarily been studied for their xenobiotic efflux, because their overexpression in cancer cells leads to drug resistance (Szakacs et al., 2006; Chen and Tiwari, 2011; Cole, 2014). However, in addition to effluxing drugs, these transporters can also contribute to disease by moving signaling molecules that govern morphogenetic behaviors of cells (Fletcher et al., 2010; Henderson et al., 2011; Jin et al., 2014; van de Ven et al., 2008).

We previously demonstrated that MDR ABC transporters are extensively expressed during embryogenesis (Goldstone et al., 2006; Shipp and Hamdoun, 2012). Among these ABC transporters, ABCC5 (also known as MRP5, MOAT-C, pABC11, sMRP) is unique in that, although being related to proteins involved in protective efflux and drug resistance (Belinsky et al., 1998; Chen and Tiwari, 2011; Kool et al., 1997; McAleer et al., 1999), it has not been demonstrated to be toxicologically important (Chen and Tiwari, 2011; Leslie et al., 2001). That ABCC5 effluxes cGMP and cAMP has long been known (Jedlitschky et al., 2000; Sager and Ravna, 2009; Wielinga et al., 2003); however, more recently, heme (Korolnek et al., 2014) and N-lactoyl-amino acids (Jansen et al., 2015) were reported to be possible substrates. Hyaluronan may also be transported by ABCC5 (Schulz et al., 2007), although it is more likely that it is translocated by hyaluronan synthase itself (Medina et al., 2012). Overall, the function of ABCC5 remains unclear.

Our previous study indicated that a sea urchin homolog of ABCC5, *Strongylocentrotus purpuratus* (*Sp*)-ABCC5a (C5a), may be expressed in non-skeletogenic mesenchyme (NSM) cells and that its subcellular localization and the timing of its expression suggest a possible developmental function (Shipp and Hamdoun, 2012). NSM cells are specified by Delta/Notch (D/N) signaling, and subsets of these cells differentiate into pigment cells, blastocoelar cells, circumesophageal muscle cells and coelomic pouch cells (Materna and Davidson, 2012; Sherwood and McClay, 1999; Sweet et al., 2002). Blastocoelar cells are derived from the oral NSM, whereas the aboral NSM gives rise to pigment cells (Ruffins and Ettensohn, 1996). Both pigment and blastocoelar cells generate larval immunocytes (Solek et al., 2013), but their regulatory states are distinct (Materna et al., 2013; Solek et al., 2013).

Marine Biology Research Division, Scripps Institution of Oceanography, University of California, San Diego, 9500 Gilman Drive, La Jolla, CA 92093-0202, USA. *Present address: Molecular Neurobiology Laboratory, Salk Institute for Biological Studies, La Jolla, CA 92037, USA. ‡Present address: Department of Molecular and Cell Biology, University of California, Berkeley, Berkeley, CA 94720, USA.

§Author for correspondence (hamdoun@ucsd.edu)

Received 5 May 2015; Accepted 14 August 2015

Development (2015) 142, 3537-3548 doi:10.1242/dev.126144

The timing of *C5a* expression, with mRNA levels peaking just after gastrulation, is coincident with a tenfold increase in levels of the ABCC5 substrate cAMP, from 2 fmol/embryo in mid-gastrulae to ~20 fmol/larva in prism/early plutei (Soliman, 1984). However, despite high cAMP levels in gastrulae and plutei, as well as increased expression of the gene encoding cAMP-dependent protein kinase (*Sp*-CAPK/PKA) (Wei et al., 2006), activity of CAPK/PKA is low at these stages (Fujino and Yasumasu, 1981). This temporal uncoupling of cAMP levels and activity of CAPK/PKA (which is enriched in pigment cells; Rast et al., 2002) suggests that after gastrulation, cAMP has additional targets beyond CAPK.

Here, we use knockdown, transporter expression, efflux assays and long-term imaging to dissect the function of C5a. We find that consistent with a developmental role, C5a is less 'promiscuous' than other MDR transporters and appears to have a narrower range of substrates. C5a is expressed in aboral NSM cells during and after gastrulation, and it is regulated by D/N signaling emanating from the skeletogenic mesoderm (SM). Morpholino antisense oligonucleotide (MASO) knockdown of C5a does not block pigment cell differentiation but alters late stages of invagination, causing prolapse of the hindgut. This prolapse is rescued with the mammalian ABCC5 substrate cAMP, and cAMP produced by soluble adenylyl cyclase (sAC) in pigment cells mediates gut invagination. Collectively, these results advance understanding of ABCC5 and shed light on signaling in gastrulation.

RESULTS

C5a is a 210 kDa protein similar to human ABCC5

The predicted tertiary structure of C5a is similar to that of *Homo sapiens* (*Hs*)-ABCC5 (Fig. 1A) (Leslie et al., 2001). C5a has two membrane spanning domains (MSDs), each consisting of six transmembrane helices (TMHs) connected by extracellular loops (ELs) and cytoplasmic loops (CLs). Two intracellular nucleotide (i.e. ATP)-binding domains (NBDs) contain canonical Walker A,

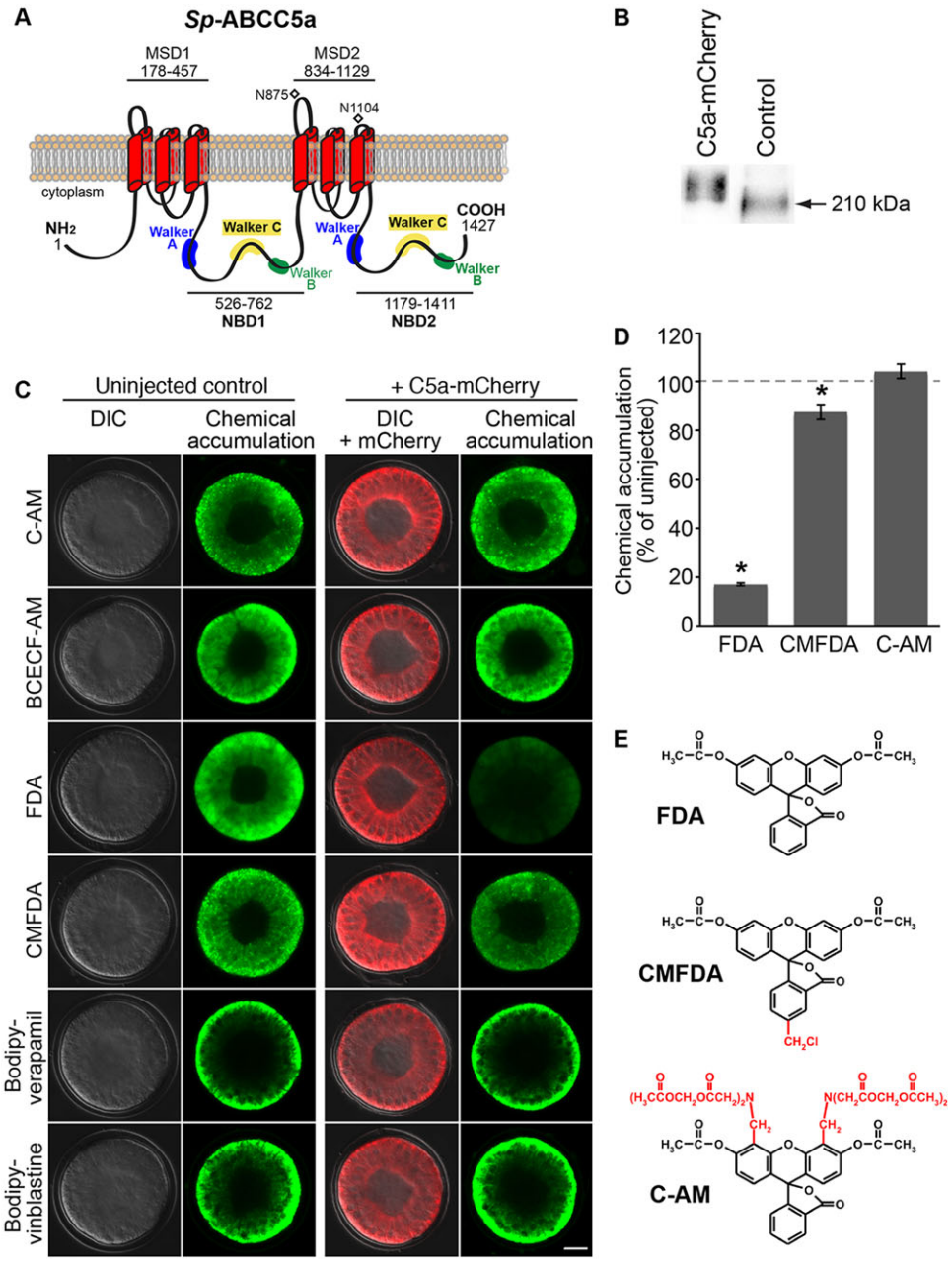

Fig. 1. C5a is a 210 kDa membrane protein that is not a broad chemical transporter. (A) Topology model of C5a in a cell membrane. Predicted glycosylation sites are numbered and marked with diamonds. (B) Protein levels in 70 hpf embryos showing overexpressed C5a (C5a-mCherry; ten embryos per lane) and endogenous C5a (control; 200 embryos per lane). (C) Representative micrographs showing accumulation of fluorone-based and bodipy-conjugated chemicals (green) in uninjected (differential interference contrast, DIC) and C5a-mCherry-overexpressing (red; DIC +mCherry) embryos. Scale bar: 20 µm. (D) Mean accumulation (±s.e.m.) of FDA, C-AM and CMFDA in C5a-overexpressing embryos. $n \geq 3$ batches (six embryos per batch); Tukey–Kramer comparison shows significant difference from uninjected control, $^{*}P \leq 0.05$. (E) Structures of the dyes in D.

Development (2015) 142, 3537-3548 doi:10.1242/dev.126144

Walker B and Walker C domains (Fig. 1A; Gökirmak et al., 2012). As with *Hs*-ABCC5, C5a lacks the N-terminal MSD0 characteristic of 'long' ABCC transporters (such as ABCC1; also known as MRP1) (Leslie et al., 2001) and is instead similar in topology to *Sp*-ABCB1a (also known as P-glycoprotein, P-gp) (Gökirmak et al., 2012). Endogenous C5a has a molecular weight of ∼210 kDa, whereas recombinant C5a-mCherry runs as a ∼230 kDa doublet, consistent with the addition of the 28 kDa mCherry tag (Fig. 1B; Fig. S1). Our antibody also recognized an 80 kDa band throughout development; however, detection of this band was inconsistent with the timing, molecular weight and morpholino knockdown of C5a expression, indicating that it was not C5a (Fig. S1). Non-specific immunoreactivity was subsequently removed by adsorption of the antisera to early embryos, prior to immunolocalization experiments (supplementary materials and methods).

C5a strongly effluxes fluorescein diacetate but not other fluorone or bodipy substrates

In most organisms, ABCC (MRP-type) transporters efflux a range of structurally diverse compounds, including signaling molecules (reviewed by Chen and Tiwari, 2011), toxicants (Bošnjak et al., 2009) and fluorescent dyes (Gökirmak et al., 2012, 2014; Litman et al., 2001; Strouse et al., 2013). In blastula-stage embryos exposed to fluorescent compounds, we find that overexpression of C5a strongly reduces accumulation of fluorescein diacetate (FDA), but not 5-chloromethylfluorescein diacetate (CMFDA), calcein acetoxymethyl ester (calcein-AM, C-AM), 2′,7′-bis-(2-carboxyethyl)-5-(and-6)-carboxyfluorescein-acetoxymethyl ester (BCECF-AM), bodipy-verapamil (b-Ver) or bodipy-vinblastine (b-Vin) (Fig. 1C), suggesting that C5a is less promiscuous than typical xenobiotic transporters (Gökirmak et al., 2014). C5a-overexpressing embryos accumulate just 17.1% (s.e.m.: 0.63) of FDA levels measured in uninjected control embryos, as quantified by FDA fluorescence (Fig. 1D). C5a-overexpressing embryos weakly but significantly efflux CMFDA, an FDA analog that is conjugated to glutathione prior to efflux (McAleer et al., 1999), accumulating 87.8% (s.e.m.: 3.06) of control CMFDA (Fig. 1D). Despite the structural similarities of FDA, CMFDA and C-AM (Fig. 1E), accumulation of C-AM is not affected by C5a overexpression (Fig. 1D). Overexpression of C5a also does not reduce accumulation of BCECF-AM, b-VER or b-VIN (Fig. 1C).

C5a expression is highest during and immediately following gastrulation

Consistent with our previous report (Shipp and Hamdoun, 2012), C5a mRNA is first detected at hatching [21 hours post fertilization (hpf)] and increases throughout gastrulation (Fig. 2A). *C5a* transcript levels peak at the late gastrula stage (42 hpf) with a 9.4-fold (±2.6) increase compared with those observed at the hatching stage, and transcript levels decrease from late gastrula to pluteus (74 hpf), with pluteus stage transcripts measuring 2.2-fold (±0.7) of hatching levels (Fig. 2A). C5a protein levels follow those of the mRNA, with an 8-h delay presumably reflecting the time needed for synthesis (Fig. 2A,B). C5a protein is first reliably detected during early gastrulation [34 hpf; 48.9±13.5 arbitrary intensity units (AIU)], and its levels increase throughout gastrulation, peaking at the prism stage (50 hpf; 79.3±13.3 AIU). C5a protein levels then decrease from prism to pluteus stage (74 hpf; 38.2±13.0 AIU).

C5a is expressed in pigment cell precursors

C5a is expressed in mesenchyme blastulae in a subset of vegetal cells likely to be NSM (Shipp and Hamdoun, 2012). Because two waves of D/N signaling specify the NSM (Materna and Davidson, 2012), we reasoned that *C5a* expression might be dependent on one of these waves. In the D/N signaling waves, the Notch ligand in NSM is activated by the Delta signal from either the SM (first wave) or a subset of the NSM (second wave) (Materna and Davidson, 2012). By exposing embryos to the γ-secretase inhibitor N-[N-(3,5-difluorophenacetyl)-L-alanyl]-S-phenylglycine t-butyl ester (DAPT) at 3 hpf and 17 hpf, Notch signaling is inhibited at the onset of either of the two waves. DAPT treatment at 3 hpf ($P \leq 0.008$), but not 17 hpf ($P \leq 0.32$), blocks *C5a* expression (Fig. 2C). This indicates that Delta signaling emanating from the SM is necessary for induction of *C5a* expression, which is consistent with *C5a* being expressed in NSM. In the aboral NSM, *glial cells missing* (*gcm*) is the primary target of D/N signaling (Materna et al., 2013; Ransick and Davidson, 2006). Knockdown of Gcm blocks expression of *C5a* ($P \leq 0.0001$; Fig. 2C), indicating that *C5a* is induced downstream of Gcm.

In mesenchyme blastulae, *C5a* transcripts colocalize with those of *gcm* (Fig. 3A), which marks aboral NSM, the pigment cell precursors (Materna et al., 2013; Ransick and Davidson, 2006). By contrast, *prox1*-expressing cells (blastocoelar cell precursors) (Materna et al., 2013) have little or no expression of *C5a* and *gcm* (Fig. 3A). A subset of *gcm*-positive cells also express C5a protein, as shown in a mid-gastrula stage embryo (Fig. 3B) and prism stage embryos (Fig. S1B,C).

Collectively, these results indicate that C5a is expressed in pigment cells and their precursors. Pigment cells are mesodermal immunocytes (Solek et al., 2013) that emerge from the archenteron during gastrulation and distribute throughout the aboral ectoderm (Gibson and Burke, 1985, 1987; Ransick and Davidson, 2006).

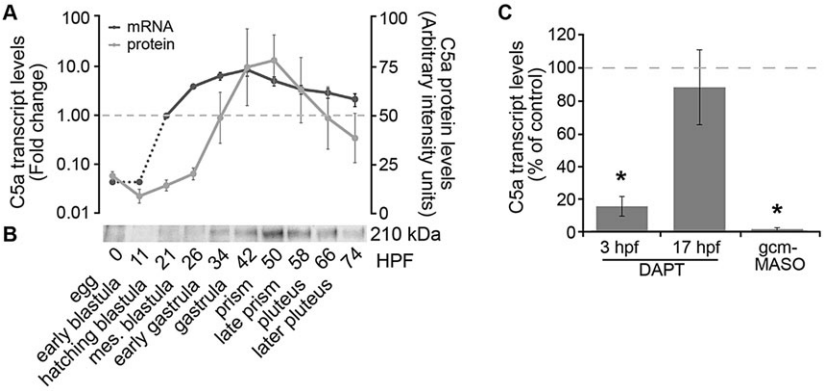

Fig. 2. Expression of C5a peaks after gastrulation and is controlled by Delta/Notch signaling from the SM. (A) Mean levels (±s.e.m.) of C5a mRNA (dark gray, left axis; fold change relative to hatching blastula) and protein (light gray, right axis) at different developmental stages (indicated in panel B). *n*=4. (B) Representative western blot (200 embryos per lane) showing protein expression at different developmental stages. (C) Gastrula-stage *C5a* gene expression in response to D/N inhibition by DAPT or Gcm knockdown. Embryos were treated with DAPT at 3 hpf or 17 hpf, or injected with Gcm-MASO. Transcript levels were calculated as fold change with respect to hatching-stage control (DMSO treated or uninjected), and data are shown as mean percent (±s.e.m.) of control fold-change (gastrula-stage). *n*=3; Tukey–Kramer comparison shows significant difference from control, *$P \leq 0.05$.

Development (2015) 142, 3537-3548 doi:10.1242/dev.126144

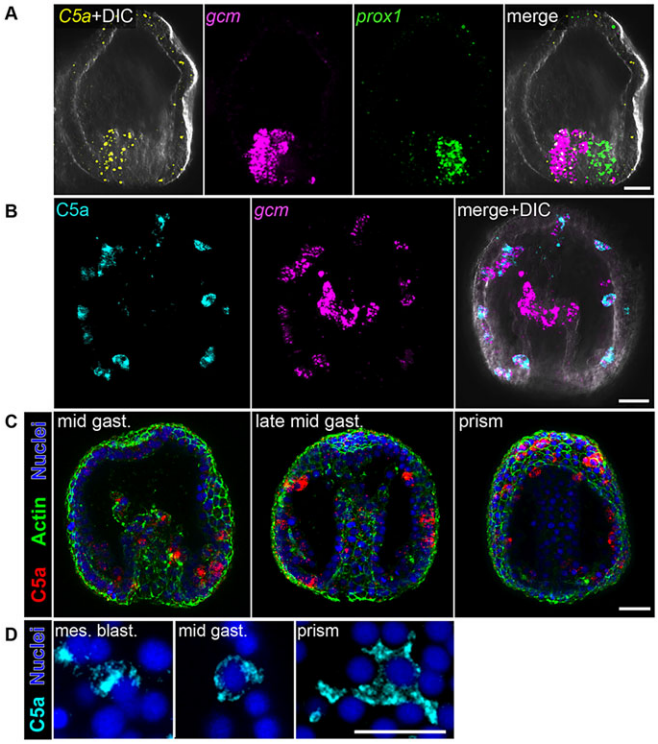

Fig. 3. C5a is expressed in pigment cells that migrate away from the archenteron during early gastrulation. (A) Localization of *C5a* mRNA (yellow) with markers of aboral (*gcm*, magenta) and oral (*prox1*, green) NSM, shown by FISH in a mesenchyme blastula embryo. (B) Protein expression of C5a (cyan; immunolabeled) with a marker of aboral NSM (*gcm*, magenta; FISH) in a mid-gastrula-stage embryo. (C) Distribution of C5a-expressing pigment cells within the embryo, shown throughout gastrulation. C5a (red) is immunolabeled, phalloidin marks actin (green) and Hoechst marks nuclei (blue). (D) Subcellular localization of C5a (cyan; immunolabeled) from mesenchyme blastula to just after gastrulation (prism). C5a-expressing cells are located in their respective embryos as follows: ingressing from vegetal pole in the mesenchyme blastula; embedding in aboral ectoderm in the mid-gastrula; moving within aboral ectoderm in the prism. Scale bars: 20 µm.

Cells expressing C5a protein ingress during early gastrulation (Fig. 3C), and by mid/late gastrulation, they are no longer associated with the archenteron but have migrated across the blastocoel to embed in the epithelium. By the prism stage, C5a-expressing cells are distributed throughout the aboral ectoderm (Fig. 3C,D), consistent in morphology and location with pigment cells (Gibson and Burke, 1985; Gustafson and Wolpert, 1967; Materna and Davidson, 2012; Ransick and Davidson, 2006).

In the transition from mesenchyme blastula to mid-gastrula stages, C5a moves from intracellular compartments to the plasma membrane (Fig. 3D). In mesenchyme blastulae, ingressing pigment cells primarily have intracellular C5a protein (Fig. 3D). Notably, at this stage C5a is undetectable by western blot (Fig. 2B). By the mid-gastrula stage, some C5a is intracellular and some has moved to the plasma membrane of pigment cells embedded in the ectoderm (Fig. 3D). By the prism stage, pigment cells extend motile pseudopodia (Gibson and Burke, 1987; Gustafson and Wolpert, 1967), and C5a is localized both intracellularly and along the plasma membrane of these projections (Fig. 3D).

C5a expression is required for gut morphogenesis, but not pigment cell formation

Two non-overlapping translation-blocking MASOs (Fig. S2A) knock down C5a expression to levels that are undetectable on western blots (Fig. S1A). In embryos injected with either MASO1 or MASO2, a protrusion (or prolapse) of the gut is seen by the pluteus stage (Fig. S2C), indicating that expression of C5a is necessary for gut morphogenesis. The two MASO-induced phenotypes are indistinguishable, and results from MASO1 are shown throughout the remaining experiments.

Given that C5a is expressed in pigment cells, we hypothesized that knockdown of this protein might affect pigment cell formation. By contrast, pigment cells differentiate and produce echinochrome pigment (Griffiths, 1965) after C5a knockdown, suggesting that C5a is not essential for pigment cell formation. Pigment cells of C5a knockdown embryos often distribute around the aboral ectoderm in similar patterns to those observed in controls (Fig. 4Ai,Bi). However, in C5a knockdown embryos, pigment cell pseudopodia and positioning relative to the ectoderm may be altered. In control embryos, pigment cells have long pseudopodial extensions and are embedded within the ectoderm such that they are in contact with the external environment (Fig. 4Ai). In C5a knockdown embryos, pigment cells have reduced pseudopodia and often fail to embed completely (Fig. 4Bi), positioning themselves sub-ectodermally as in normal development several hours earlier (Ransick and Davidson, 2006).

C5a expression is required for orientation of the hindgut

Because the most robust phenotype in C5a knockdown embryos is prolapse of the gut (Fig. 4Bii-iv), we measured the timing and frequency of gut prolapse after knockdown. Prior to gastrulation, few, if any, abnormalities are evident in knockdown embryos (Fig. 4C,D) apart from a slight developmental delay commonly seen with MASOs in sea urchins. At 36 hpf, ≥93% (±7) of knockdown embryos are indistinguishable from controls (Fig. 4C,D). By 48 hpf, control embryos are full gastrulae, and 59% (±26) of C5a knockdown embryos have abnormal elongation of the vegetal pole (Fig. 4C,D). Nineteen percent (±10) of embryos have only a mild prolapse, and 40% (±17) have a moderate/severe prolapse (Fig. 4D).

At 60 hpf, prism-stage control embryos have growing skeletal rods and extended archenterons that may be beginning to differentiate into gut compartments (Fig. 4C). At this time, 90% (±6) of C5a knockdown embryos have a clear prolapse of the gut; 77% (±10) of knockdowns have a moderate/severe prolapse, and 13% (±8) have a flare/mild prolapse (Fig. 4D). In some cases, we also observe absence or deformation of skeletal rods. Fig. 4C shows a 60 hpf moderate hindgut prolapse. By the 72 hpf pluteus stage, control embryos have elongated skeletal rods, a tripartite gut, and a fused mouth (Fig. 4C). In C5a knockdown embryos, the severity of prolapse and degree of skeletal formation vary: 80% (±5) of knockdowns have a moderate/severe prolapse, and a small percent (4%±2) of embryos have guts that become everted into exogastrulae (Fig. 4D). Fig. 4C shows a severe prolapse, where the gut has collapsed against the oral/ventral wall of the embryo.

Finally, a scanning electron micrograph of a C5a knockdown embryo shows a difference in ciliation of ectoderm tissue versus the prolapsed tissue (Fig. 4E). The ectoderm is covered in long, uniform cilia, but these long cilia are absent from the prolapsed tissue, suggesting that the prolapse is not composed of ectoderm but is instead formed from endoderm.

Live cell confocal time-lapse imaging of C5a morphants

To define the nature of the defect induced by removal of C5a, live cell confocal time-lapse movies were used to study changes in

Development (2015) 142, 3537-3548 doi:10.1242/dev.126144

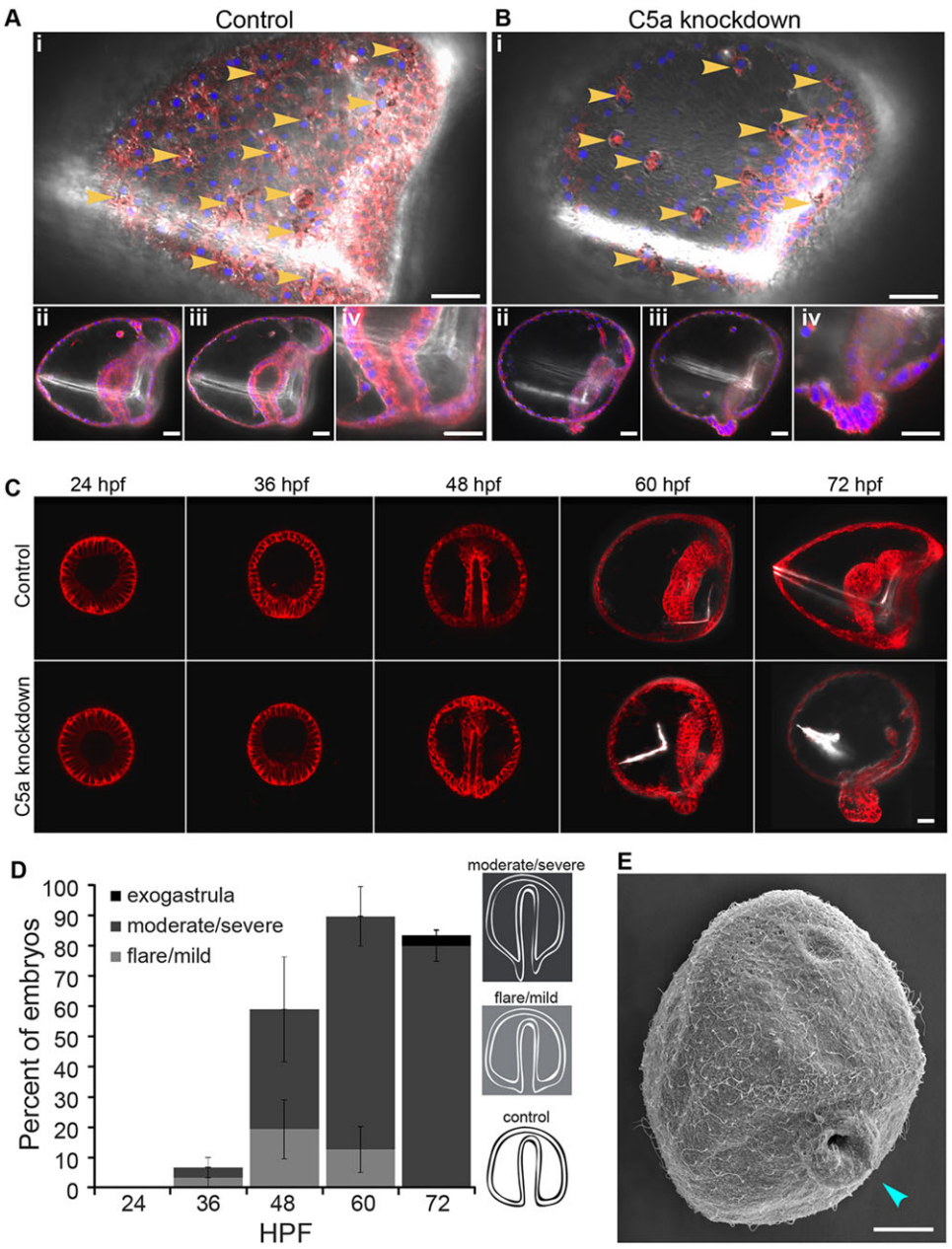

Fig. 4. Gut prolapse is the major morphology in C5a knockdown embryos. (A,B) Overview of the C5a-MASO phenotype. A control embryo (A) and C5a knockdown embryo (B) are shown. Membranes (red) and nuclei (blue) are labeled with LCK-mCherry and H2B-CFP. Shown are: (i) distribution of pigment cells (yellow arrowheads) within the aboral ectoderm; (ii,iii) two deeper cross-sections showing gut and skeleton morphology; and (iv) higher magnification view of the hindgut region. (C) A time-course of the C5a knockdown phenotype is shown from 24 to 72 hpf with representative embryos. Membranes (red) are labeled with LCK-mCherry. (D) Mean (±s.e.m.) frequency of prolapse in C5a knockdown embryos from 24 to 72 hpf. Schematics depict the moderate/severe (dark gray) and flare/mild (light gray) categories. *n*=3 batches (55 embryos total). (E) Scanning electron micrograph of a representative C5a knockdown embryo at 60 hpf. The invaginated stomodeum (mouth) is at the top, and the prolapsed anus (blue arrowhead) is at the base of the image. Scale bars: 20 µm.

morphology through development of C5a knockdown embryos. In these embryos, the archenteron tips make contact with the stomodeums, and mesenchyme cells migrate across blastocoels (Fig. 5). In embryo 5 of Movie 1 (Fig. 5A), SM cells assume their appropriate places on either side of the vegetal pole. Hindgut prolapses are evident after the archenterons have elongated (Fig. 5A), distinguishing between this phenotype and typical exogastrulation.

In Movie 2 (Fig. 5B), a control and a C5a knockdown embryo are shown side by side following the completion of gastrulation. The control embryo is spheroid in shape, as the hindgut remains flush with the vegetal pole ectoderm (yellow arrowhead). In the C5a knockdown embryo, the gut prolapses to create a protrusion from the vegetal pole (yellow arrowhead). This protrusion is shown in cross-section in Movie 3 (Fig. 5C), and isosurface rendering of this embryo highlights movements of NSM filopodia. At the beginning of the experiment, the archenteron is elongated and oriented towards the presumptive oral hood. Only a subtle thickening is seen at the vegetal pole. Within 1 h (1 s of movie), the archenteron tip has successfully oriented itself to contact the presumptive stomodeum beneath the oral hood. NSM cells delaminate from the archenteron and migrate across the blastocoel. The vegetal pole continues to thicken, and, as the archenteron elongates, the hindgut protrudes. The site that should become the anal sphincter is visible at the interface between the thinner ectoderm cells and the thicker gut cells of the prolapse (Fig. 5C, yellow arrowheads).

C5a-mediated prolapse is rescued by cAMP

Because mammalian ABCC5 transports cyclic nucleotides (Jedlitschky et al., 2000; Sager and Ravna, 2009; Wielinga et al., 2003), and there is evidence for cAMP signaling in C5a-expressing pigment cells (i.e. expression of *Sp*-CAPK/PKA; Rast et al., 2002), we tested whether there is a link between cyclic nucleotide signaling and C5a. When mesenchyme blastulae are exposed to the membrane-permeable cyclic nucleotide analogs pCPT-cAMP or pCPT-cGMP, the hindguts hyper-invaginate (Fig. 6A). Exposing

Development (2015) 142, 3537-3548 doi:10.1242/dev.126144

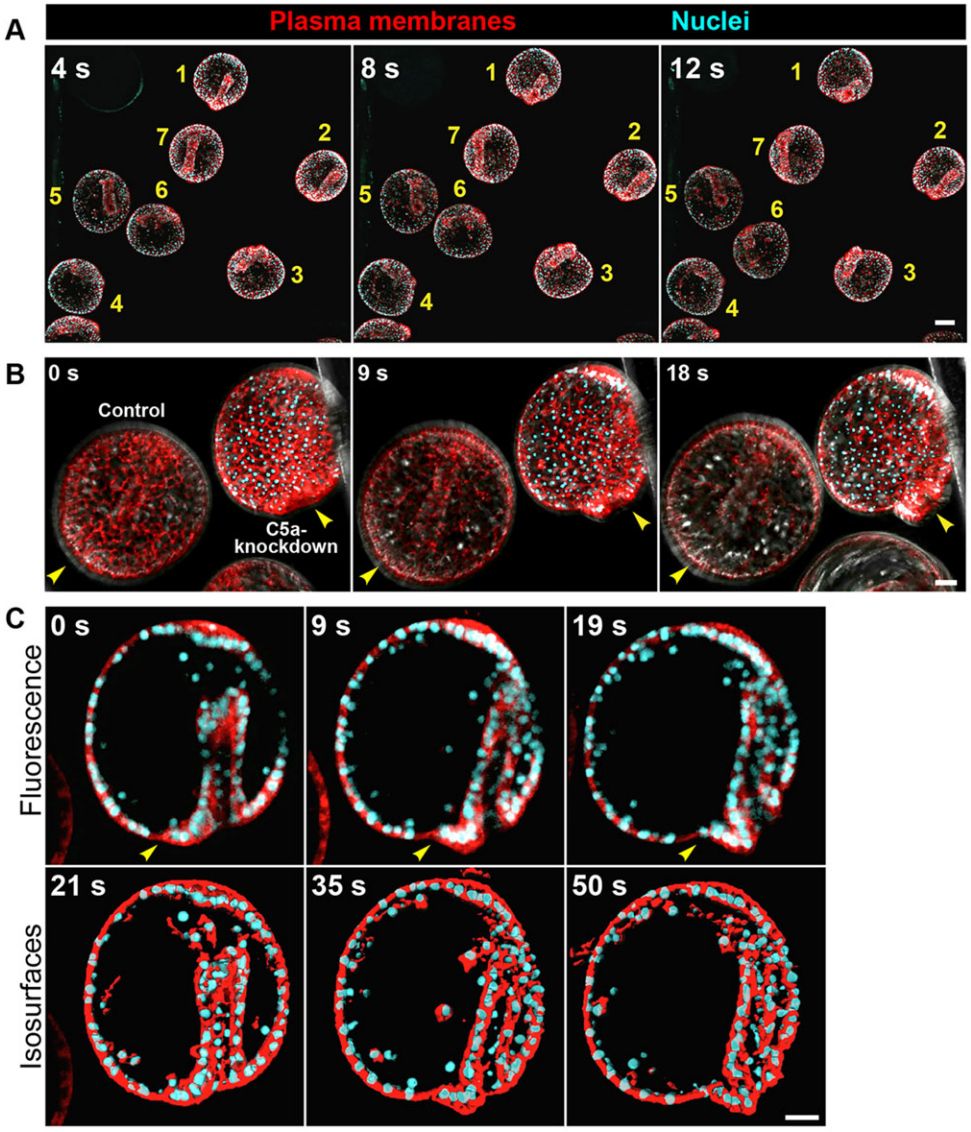

Fig. 5. Long-term imaging of C5a knockdown embryos reveals defects in hindgut formation. Long-term time-lapses are shown as still shots from Movies 1-3. Images are labeled with the corresponding time (seconds) on the movie. In all movies, membranes (red) are labeled with LCK-mCherry, and nuclei (blue) are labeled with H2B-CFP. (A) Stills from Movie 1. Maximum intensity projections (MIPs) of seven C5a knockdown embryos. (B) Stills from Movie 2. MIPs of a control embryo (membrane labeled only) and a C5a knockdown embryo (membrane and nuclei labeled) shown side by side. Vegetal poles are indicated with yellow arrowheads. (C) Stills from Movie 3. Cross-sections of the C5a knockdown embryo from Movie 2. The same three time points are shown both as raw fluorescence and as isosurfaces. Yellow arrowheads indicate the presumptive site of the anal sphincter. Scale bars: 50 µm (A); 20 µm (B,C).

C5a knockdown embryos to these analogs rescues hindgut prolapse (Fig. 6A) in a dose-dependent manner (Fig. 6B,C). The percentage of embryos that prolapse (84%±7 in controls) is significantly reduced ($P \leq 0.05$) in the presence of 25 µM (45%±7) or 100 µM (18%±2) cGMP (Fig. 6B). However, cAMP is more potent than cGMP and reduces the frequency of prolapse from 90% (±4) in controls to 72% (±14) at 1 µM, 29% (±14) at 10 µM, and 13% (±8) at 20 µM (Fig. 6C).

cAMP necessary for gut invagination is derived from sAC in pigment cells

As exogenous cAMP appears to enhance invagination, we examined the source of endogenous cAMP. cAMP is produced by soluble adenylyl cyclase (sAC) and transmembrane adenylyl cyclase (tmAC), and these enzymes can be specifically inhibited with 2-(1H-benzimidazol-2-ylthio)-2-[(5-bromo-2-hydroxyphenyl) methylene]hydrazide, propanoic acid (KH7) and 2′,5′-dideoxyadenosine, respectively (Beltrán et al., 2007; Tresguerres et al., 2011). In embryos exposed to these inhibitors, gut formation is impaired with 10 µM KH7, but not 100 µM 2′,5′-dideoxyadenosine (Fig. 6D), indicating that sAC-produced cAMP is necessary for gastrulation. In addition, *sAC* gene expression (Fig. 6E,F) parallels that of *C5a* (Fig. 2A; Fig. 3A,B) in that *sAC* mRNA localizes to *gcm*-expressing pigment cells (Fig. 6E), and mRNA levels peak just after gastrulation (Fig. 6F).

C5a transports FDA out of pigment cells, then FDA accumulates in the gut

Because FDA is a substrate of C5a (Fig. 1C,D), we assessed FDA accumulation in embryos after gastrulation (Fig. 7). At the prism stage, pigment cells can be definitively identified by confocal microscopy with echinochrome autofluorescence. In control embryos from gastrula to pluteus stages, FDA accumulates less in pigment cells than in neighboring ectoderm cells (Fig. 7A). In late gastrula controls, when pigment is not yet visible, FDA is excluded from cells that are located where pigment cells normally reside. By contrast, in C5a knockdown embryos, pigment cells accumulate FDA at levels comparable to those of neighboring cells (Fig. 7B). Together, these observations indicate that C5a effluxes FDA from pigment cells. As large vesicles of FDA are not abundant in control embryo pigment cells (Fig. 7Aiii), this also suggests that the major C5a transport activity is from plasma membrane and not intracellular C5a. Additionally, in both control and C5a knockdown embryos, FDA accumulates strongly in the

Development (2015) 142, 3537-3548 doi:10.1242/dev.126144

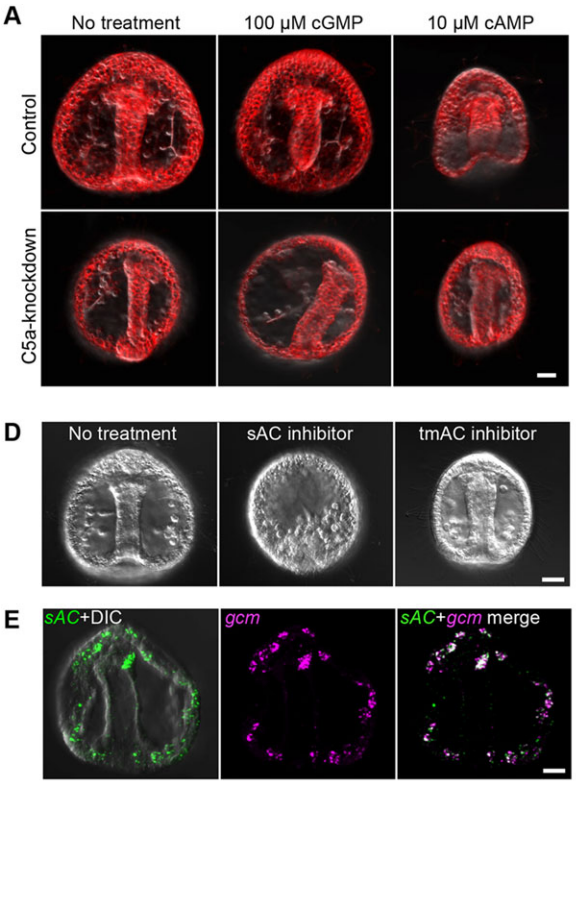

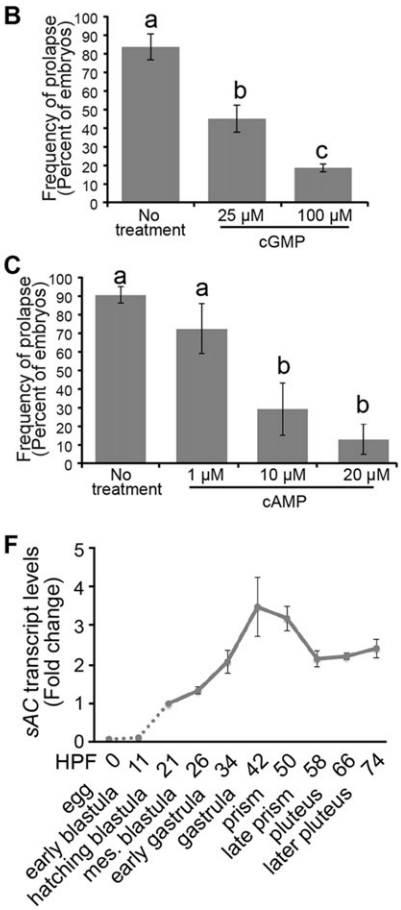

Fig. 6. C5a knockdown-mediated prolapse is rescued by cAMP, which is derived from sAC in pigment cells. (A) Control and C5a knockdown embryos treated at the mesenchyme blastula stage with pCPT-cGMP or pCPT-cAMP, and imaged at the 68 hpf pluteus stage (oral view). Membranes (red; pseudocolored) are labeled with LCK-mCitrine. (B,C) Mean (±s.e.m.) frequency of prolapse in C5a knockdown embryos treated with pCPT-cGMP (B) or pCPT-cAMP (C). Morphologies of 45-73 embryos from four to five batches per treatment were assessed at the 68 hpf pluteus stage, and any hindgut defect (mild to severe) was counted as prolapsed. $n \geq 4$ batches; one-way ANOVA with Tukey–Kramer post-hoc comparison shows significance (groups with different letters are statistically different from one another; $P \leq 0.05$). (D) cAMP production was perturbed by treating mesenchyme blastulae with the adenylyl cyclase inhibitors KH7 (10 µM; sAC specific) and 2′,5′-dideoxyadenosine (100 µM; tmAC specific). Prism embryos (48 hpf) are shown. (E) Localization of *sAC* mRNA (green) with a marker of aboral NSM (*gcm*, magenta), shown by FISH in a gastrula embryo. (F) Mean levels (±s.e.m.) of *sAC* mRNA at different developmental stages (fold change relative to hatching blastula). $n=3$. Scale bars: 20 µm.

gut (Fig. 7C), suggesting that the gut imports C5a substrates, has low MDR efflux activity, or both.

DISCUSSION

ABC transporters are extensively utilized by the embryo (Goldstone et al., 2006; Gökirmak et al., 2014; Shipp and Hamdoun, 2012), yet most of their functions remain unknown. Although some MDR transporters play important roles in xenobiotic efflux, others are more likely to have ancestral roles in sensing and signaling (Nigam, 2015). Here, we report a novel developmental function for C5a in morphogenesis. This protein is expressed in migratory pigment cells, which are immunocytes derived from mesoderm, and knockdown of C5a leads to gut defects, including prolapse from the blastopore after gastrulation. The ABCC5 substrate cAMP mediates invagination, causing hyper-invagination in control embryos, and rescuing the prolapse phenotype in C5a knockdown embryos. Inhibition of sAC, which generates cAMP in pigment cells, blocks gut formation. Together, these data support a model in which C5a-mediated efflux of sAC-derived cAMP from pigment cells controls late invagination of the hindgut (Fig. 8).

Substrates of C5a

Consistent with its developmental role, C5a has narrower substrate selectivity than other sea urchin multidrug resistance protein (MRP/ABCC) transporters. For example, *Sp*-ABCC1, like C5a, is an MRP that localizes to basolateral membranes when overexpressed in sea urchin embryos. Unlike C5a, ABCC1 effluxes a wide variety of compounds, including C-AM, BCECF-AM, Fluo3-AM, CMFDA, FDA, b-Vin, and members of the cyanine and anthracene dye families (Gökirmak et al., 2014). Of the six substrates we tested here (four fluorones and two bodipy conjugates), only FDA is strongly effluxed by C5a.

A number of studies have shown that mammalian ABCC5 transports cyclic nucleotides (Boadu and Sager, 2004; Jedlitschky et al., 2000; Meyer Zu Schwabedissen et al., 2005; Sager and Ravna, 2009; Sager et al., 2012; Wielinga et al., 2003; Wijnholds et al., 2000). cGMP is reported to be a higher-affinity substrate than cAMP, but the exact affinity of cGMP remains unclear (de Wolf et al., 2007; Pratt et al., 2005; Reid et al., 2003; Wielinga et al., 2003). We find that although both pCPT-cGMP and pCPT-cAMP rescue the C5a knockdown phenotype, cAMP is effective at lower concentrations than cGMP. Additionally, sAC activity, cAMP and C5a are all necessary for gut development, together suggesting that in sea urchins, cAMP is the relevant C5a substrate mediating hindgut morphogenesis. As cAMP and cGMP are structurally similar, the rescue by cGMP may be caused by off-target effects on cAMP-responsive pathways, or there may be an additional and/or synergistic role for cGMP.

C5a is expressed in motile pigment cells but is necessary for gastrulation

Although C5a is expressed in pigment cells and is downstream of Gcm, it does not appear to be required for pigment cell differentiation. C5a knockdown embryos have echinochrome-containing pigment cells, even in embryos with gut prolapse. Often, the positions of pigment cells in knockdown embryos – distributed around the aboral ectoderm – are similar to those of control embryos (Gibson and Burke, 1985, 1987; Ransick and Davidson, 2006), though they are positioned slightly further from the apical surface than in controls.

Development (2015) 142, 3537-3548 doi:10.1242/dev.126144

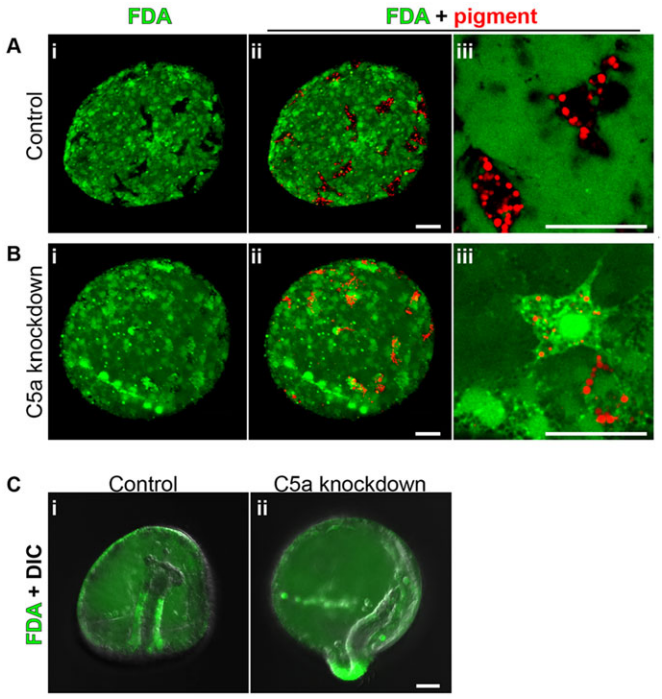

Fig. 7. C5a transports FDA out of pigment cells, and FDA is taken up by gut cells. Accumulation of FDA (green) in late prism embryos. Pigment cells are visualized with echinochrome autofluorescence (red), and representative embryos are shown. (A) A whole embryo (i,ii) and higher magnification image of two pigment cells (iii) show FDA accumulation in controls. (B) A whole embryo (i,ii) and higher magnification image of two pigment cells (iii) show FDA accumulation in C5a knockdown embryos. (C) FDA accumulation in the guts of control and C5a knockdown embryos. Scale bars: 20 µm.

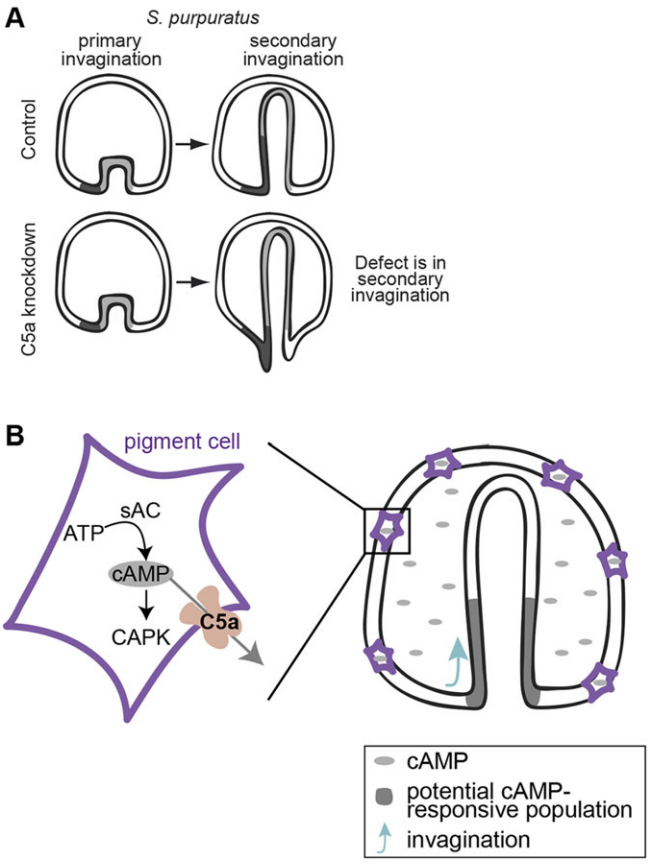

Fig. 8. A model of C5a knockdown-induced gut prolapse. (A) In *S. purpuratus*, a subset of veg1 cells contribute to the elongating archenteron late in gastrulation, during secondary invagination (Barnet, 2011; Ransick and Davidson, 1998). In C5a knockdown embryos, we observe defects in secondary invagination. (B) We propose that C5a-expressing pigment cells embed in the aboral ectoderm and transport sAC-derived cAMP into the blastocoel. This cAMP promotes hindgut invagination and orientation through an unknown mechanism.

Pigment cell specification is dependent on the Delta signal from SM cells, which activates Notch signaling in the NSM and establishes the aboral NSM gene regulatory network (GRN) (Materna and Davidson, 2012; Sherwood and McClay, 1999; Sweet et al., 2002). When we treated embryos at 3 hpf with DAPT to inhibit D/N signaling emanating from SM cells, *C5a* gene expression was blocked. Furthermore, knockdown of Gcm, the primary Notch target in aboral NSM cells (Materna et al., 2013; Ransick and Davidson, 2006), also blocked *C5a* expression, indicating that *C5a* gene expression is activated as part of the aboral NSM GRN.

Interestingly, when Gcm is knocked down by MASOs, the resulting embryos have an 'albino phenotype' lacking pigment, but defects in gut morphogenesis are less prevalent and include exogastrulation at higher MASO concentrations (Ransick and Davidson, 2006). Perturbing D/N signaling from SM, the upstream inducer of *gcm* and *C5a*, resulted in a large fraction of embryos exogastrulating, consistent with previous reports (Materna and Davidson, 2012). However, whereas C5a knockdown leads to embryos with differentiated pigment cells and prolapsed hindguts, Gcm knockdown leads to embryos with undifferentiated pigment cells and (usually) normal guts. One possibility is that the Gcm knockdown is pleiotropic and that it induces an alternative pathway that bypasses the need for C5a.

Contributions of veg-lineage cells to the gut and timing of hindgut morphogenesis

Gastrulation in sea urchin embryos varies by species with regard to timing, the angle of the archenteron, and the contributions of different cell types to the archenteron (Barnet, 2011; Hardin, 1989; Hardin and McClay, 1990; Logan and McClay, 1997). In *S. purpuratus*, the mechanism of archenteron elongation resembles that of *Lytechinus variegatus* in that some veg1 cells ultimately contribute to the archenteron (Logan and McClay, 1997; Ransick and Davidson, 1998). Very late in gastrulation, a subset of veg1 cells (*brachyury* expressing) invaginate and produce the anus/hindgut, whereas a distinct subset of veg1 cells remains a part of the vegetal ectoderm (Barnet, 2011; Gross and McClay, 2001). The timing of C5a knockdown-mediated gut prolapse is consistent with a defect in secondary invagination (Fig. 8A). Given that a subset of veg1-derived cells form the *S. purpuratus* hindgut late in gastrulation, it is likely that C5a efflux activity in pigment cells is required for proper movement and orientation of veg1-derived hindgut cells. Interestingly, pigment cells have been reported to affect gastrulation in *Echinometra mathaei* (Takata and Kominami, 2004), a sea urchin closely related to *S. purpuratus* (Smith et al., 2006). However, in *E. mathaei*, pigment cells influence gastrulation movements during primary invagination.

How does C5a in pigment cells affect the position of the hindgut?

Although we show that C5a efflux is necessary for gastrulation, and that cAMP enhances invagination, the precise link between C5a and invagination remains unknown. Based on the localization of C5a, one possibility is that intracellular C5a could play some role in

Development (2015) 142, 3537-3548 doi:10.1242/dev.126144

autonomous regulation of pigment cells. However, given the observations that pigment cells transport FDA out of cells through C5a, and that the most prominent effect of C5a knockdown is non-autonomous, the most plausible explanation is that plasma membrane-localized C5a transports a signal to the hindgut, and we propose that this signal may be cAMP (Fig. 8B). Consistent with this idea, gut cells accumulate FDA, suggesting that these cells could also take up C5a's endogenous substrates. cAMP uptake has been reported in prokaryotes (Ammerman and Azam, 1982) and eukaryotes (Francko, 1989), but such a finding in deuterostome gut morphogenesis would be novel.

It is also possible that extracellular cAMP could function via G protein-coupled receptors (GPCRs) on basal gut membranes to induce invagination. cAMP can activate GPCRs directly (Miranda et al., 2015) or can first be metabolized extracellularly to adenosine (Godinho et al., 2015). In *Dictyostelium* development, cAMP secreted by ABC transporters stimulates chemotaxis (Miranda et al., 2015), and chemotaxis is an important mechanism of cell movement during deuterostome gastrulation (Dormann and Weijer, 2006). Through either surface or intracellular activity, cAMP could trigger alterations in gut cell adhesion, polarity and/or chemokinesis. Consequently, the absence of cAMP efflux in C5a knockdown embryos may compromise the orientation of late-invaginating cells, leading them to fold outwards as a consequence of gut elongation.

Finally, it is interesting to note that a phenotype similar to our observed hindgut prolapse was reported by Burke et al. (1991), which was caused by antibodies disrupting apical lamina glycoproteins (fibropellins; Burke et al., 1998). A connection between C5a activity, pigment cell embedding, and the apical lamina is currently unclear, but it is conceivable that perturbing pigment cell embedding may change the landscape of ectoderm adhesion molecules. This could modify biophysical properties of invagination and/or amplify the effect caused by altered cAMP signaling.

Evolutionary implications of C5a-mediated gut morphogenesis

ABCC transporters often exhibit one-to-one orthology across broad phylogenetic spans (Goldstone et al., 2006; Whalen et al., 2012). For example, zebrafish, mouse and human ABCC5 are more closely related to one another than to other ABCC family members from the same organism (Korolnek et al., 2014), suggesting potential conservation of function. Consistent with this idea, *Hs*-ABCC5 has similar topology (Ravna et al., 2008; Sager et al., 2012), subcellular localization (Borst et al., 2007; Korolnek et al., 2014; Meyer Zu Schwabedissen et al., 2005; Wijnholds et al., 2000), and fluorescent substrates to sea urchin C5a. For instance, McAleer et al. (1999), showed that *Hs*-ABCC5 strongly effluxes FDA and CMFDA, but does not efflux C-AM or rhodamine dyes. Similarly, we found that C5a strongly effluxes FDA, weakly effluxes CMFDA, and does not efflux C-AM. An exception is BCECF-AM, which is moderately effluxed by *Hs*-ABCC5 (McAleer et al., 1999), but not by C5a, possibly indicating modest divergence in substrate selectivity.

This study is the first detailed characterization of an ABCC5 transporter in the development of an animal embryo. A key question raised by our work is whether the function of ABCC5 might be evolutionarily conserved. In *Caenorhabditis elegans* and *Danio rerio*, ABCC5 may transport heme, and its knockdown causes embryonic lethality and reduced blood cell formation, respectively (Korolnek et al., 2014). In *Dictyostelium* development, ABCC5 is a candidate cAMP transporter (Miranda et al., 2015). In mammals, studies of ABCC5 in development are sparse, but human ABCC5 is expressed in membranes of amniotic epithelia (Aye et al., 2007), and in cytotrophoblasts and syncytiotrophoblasts (Manceau et al., 2012; Meyer Zu Schwabedissen et al., 2005). The highly regulated expression of this transporter, and clear effects of its perturbation in embryos, underscore its potential to play a central role in developmental signaling.

MATERIALS AND METHODS

Animals and reagents

Sea urchins, *Strongylocentrotus purpuratus*, were procured as described by Shipp and Hamdoun (2012). Embryos were grown at 15°C. Stock solutions were prepared in dimethyl sulfoxide (DMSO) or Nanopure water and diluted to final concentrations in filtered seawater (FSW).

Efflux assays were performed with C-AM (Biotium); FDA (Sigma); and CMFDA, BCECF-AM, b-VER and b-VIN (all Life Technologies). The γ-secretase inhibitor DAPT (EMD Millipore) was used to assess the effects of D/N signaling on gene expression. Hoechst 33342 and Phalloidin-Alexa Fluor 488 (Life Technologies) were used to label nuclei and actin in immunolabeled embryos. Rescue experiments were performed with pCPT-cAMP and pCPT-cGMP (Sigma), and inhibition of adenylyl cyclase was performed with KH7 and 2′,5′-dideoxyadenosine (gifts from Dr. Martin Tresguerres, Scripps Institution of Oceanography, UCSD, CA, USA).

Gene expression analyses

RNA isolation, cDNA synthesis and quantitative real-time polymerase chain reaction (qPCR) were performed according to Shipp and Hamdoun (2012). Experiments were replicated with four separate batches of embryos for *C5a* and three batches for *sAC*. qPCR primers for *sAC* (SPU_012084) were: Fwd: 5′-AACTGGGACACAGAGGTTGG-3′, Rev: 5′-CCTTCAT-TGCCTATGGTCGT-3′.

To assess the effect of D/N signaling on gene expression, embryos were treated with 8 µM DAPT at 3 hpf or 17 hpf. DAPT inhibits cleavage of Notch, which blocks its ability to associate with Su(H) and activate transcription (Hughes et al., 2009; Materna and Davidson, 2012). RNA was isolated from unfertilized eggs (0 hpf; untreated), hatching blastulae (21 hpf), and gastrulae (43 hpf). *C5a* gene expression at the gastrula stage was quantified as fold change with respect to control samples at the earliest detectable stage, i.e. hatching (DMSO-treated). The experiment was replicated with three batches. The effects of Gcm knockdown on *C5a* expression were determined similarly, only with Gcm-MASO-injected embryos from three separate batches.

Fluorescence RNA *in situ* hybridization (FISH) was performed with minor modifications from published protocols. Pre-hybridization washes, hybridization, and post-hybridization washes were performed according to Shipp and Hamdoun (2012). All other steps were performed according to Chen et al. (2011). *gcm* and *prox1* probes were used to mark aboral and oral NSM, respectively (Materna et al., 2013). Primers to generate the *sAC in situ* probe were: Fwd: 5′-GATGTAGGTGAGAAGCCGTTAG-3′, Rev: 5′-CGAGGAAGAGGCAACAAGAA-3′.

Microinjection of mRNAs and MASOs

Injections and mRNA syntheses were performed as described previously (Gökirmak et al., 2012; Shipp and Hamdoun, 2012). For C5a overexpression, we injected 0.8-1 mg/ml of C-terminal mCherry-tagged C5a mRNA (C5a-mCherry). For live-imaging, LCK-mCherry, LCK-mCitrine and/or histone H2B-CFP mRNAs were injected at 0.05 mg/ml each to label membranes and nuclei.

To knock down C5a, MASOs were obtained from Gene Tools: C5a-MASO1, 5′-GAGGATCGTTGCCTTCTATAATCAT-3′ (300 µM); C5a-MASO2, 5′-TTATTTTCCCCGGCGTCATAAGTTT-3′ (500-600 µM). MASOs were co-injected with LCK-mCherry and/or histone H2B-CFP mRNA to label membranes and nuclei for live-imaging. Gcm was knocked down as described by Ransick and Davidson (2006).

Western blot

Western blots were performed as described previously (Whalen et al., 2012) with affinity-purified anti-C5a antibody (described in supplementary

Development (2015) 142, 3537-3548 doi:10.1242/dev.126144

materials and methods). For the developmental time-series, protein lysates were obtained from the same embryo batches and time points used for gene expression analyses. Western blots were run with each of the four batches independently and probed with anti-C5a. Anti-C5a was used at 1:500, and the secondary goat anti-rabbit horseradish peroxidase-conjugated antibody was used at 1:2000. The 210 kDa C5a band was quantified by densitometry with ImageJ (NIH).

Transporter efflux activity assays

Efflux assays were modified from Gökirmak et al. (2012). Briefly, uninjected (control) and C5a-CmCherry-injected (C5a overexpressing) embryos were grown to the ∼14 hpf blastula stage, then incubated and washed prior to imaging as follows: 100 nM FDA or CMFDA (60 min incubation followed by ten washes, then 30 min FSW incubation); 125 nM b-VER or b-VIN (90 min incubation followed by ten washes); 250 nM C-AM or BCECF-AM (90 min incubation). For each dye, experiments were replicated three or four times with genetically distinct batches of embryos, and six embryos were measured per batch.

To assess FDA accumulation after gastrulation, embryos were treated with 10 nM FDA for 60 min, transferred into FSW, and incubated 10 min prior to imaging.

Immunohistochemistry

Embryos were fixed in 4% paraformaldehyde for 1 h at 15°C and washed in 0.05% saponin in PBS, 50 mM glycine in PBS, and then PBS alone. Samples were blocked for 2 h at 15°C in 2% bovine serum albumin (BSA) with 5% goat serum in PBS, then washed with PBS and incubated in adsorbed anti-C5a primary antibody (described in supplementary materials and methods) at 14°C for ∼14 h. Samples that had already been processed for FISH were blocked and treated with primary antibody, bypassing the initial fixation and wash steps. Embryos were washed in PBS then incubated at 14°C in 1:1000 goat anti-rabbit Alexa Fluor 594-conjugated secondary antibody (Life Technologies) in 2% BSA-PBS. Samples were washed in PBS and stained with 10 µM Hoechst 33342 and 1.5 units/ml Phalloidin-Alexa Fluor 488 before imaging.

Quantification of C5a knockdown phenotypes and rescue

To quantify the timing of the C5a knockdown phenotype, embryos were injected with MASO1 and LCK-mCherry and/or histone H2B-CFP mRNAs for imaging. A total of 55 embryos were used from three genetically distinct batches. Embryos were individually assessed at 24, 36, 48, 60 and 70 hpf by culturing one embryo per well (Costar 96-well round bottom plate, Fisher) in 100 µl FSW. We classified gut prolapses as flare/mild, moderate/severe, or exogastrula (which was rare). Control-injected (54 embryos, LCK and/or histone mRNA only) and uninjected (56 embryos) morphologies were also monitored and quantified, both of which resulted in 100% healthy embryos (not shown).

To quantify rescue of the C5a knockdown phenotype, MASO1-injected embryos were treated with membrane-permeable pCPT-cGMP or pCPT-cAMP at the mesenchyme blastula stage. Morphologies of 45-73 embryos from four to five genetically distinct batches per treatment were assessed at the 68 hpf pluteus stage, and any hindgut defect (mild to severe) was counted as prolapsed.

Microscopy

Live imaging for efflux assays was performed as described (Gökirmak et al., 2012) using a Zeiss LSM 700 laser scanning confocal microscope [Plan-Apochromat 20× air objective, 0.8 numerical aperture (NA); Zeiss]. Intracellular dye accumulation was quantified using the 'measure' module of ImageJ. Efflux activity of C5a was determined by intracellular substrate fluorescence relative to uninjected control embryos.

To assess FDA accumulation after gastrulation, whole embryos were imaged on a Zeiss LSM 700 (Plan-Apochromat 20× air, 0.8 NA), and individual cells were imaged on a Leica Sp8 confocal microscope (Plan-Apochromat 40× water, 1.1 NA; Leica).

To characterize embryo morphology, high-resolution images were captured on a Zeiss LSM 700 microscope with a Zeiss LDC-Apochromat 40× water objective (1.1 NA), and images were processed with ImageJ. To quantify C5a knockdown phenotypes, embryos were monitored at 25-40× magnifications on a Leica M165FC stereoscope.

For FISH and immunohistochemistry, embryos were mounted in TBST (Tris-buffered saline + 0.1% Tween-20) and imaged on a Zeiss LSM 700 microscope (20× or 40× objective). Time-lapse imaging of C5a knockdown embryos is described in supplementary materials and methods (Fig. S3), and all time-lapses were processed using Imaris 7.6.1 software (Bitplane). For scanning electron microscopy, embryos were fixed at 60 hpf in 2% glutaraldehyde in FSW, then processed and imaged according to Holland and Jespersen (1973).

Statistics

Statistics were performed in JMP10 (SAS) with one-way ANOVAs and Tukey–Kramer post-hoc comparisons ($P \leq 0.05$), blocked by batch. Each batch was from one male and one female sea urchin. For efflux assays, arbitrary fluorescence units/area values were compared. For gene expression with DAPT treatment and Gcm-MASO, fold changes (with respect to control hatching stage) were compared. For pCPT-cAMP and pCPT-cGMP rescue experiments, percentages of embryos prolapsed were compared.

Acknowledgements

We are grateful to Dr Victor D. Vacquier, Dr Joseph Campanale, Jose Espinoza, Lisa Mesrop, Dr Sascha Nicklisch, Dr Stefan Materna, Hannah Rosenblatt, Boris Stepanyuk and Alysha Vu for constructive discussions and/or assistance. We thank Dr Nicholas D. Holland for performing EM, Dr Andrew Ransick for *gcm* and *prox1* FISH probes, Dr Yi-Hsien Su for FISH advice and protocols, and Dr Martin Tresguerres (Scripps Institution of Oceanography, UCSD) for adenylyl cyclase inhibitors and sAC advice. Thank you to the Achievement Rewards for College Scientists (ARCS) Foundation and Philanthropic Educational Organization (PEO) for support of L.E.S.

Competing interests

The authors declare no competing or financial interests.

Author contributions

L.E.S. and A.H. conceived and designed the experiments and wrote the manuscript. L.E.S., R.Z.H., G.W.M. and T.G. performed the experiments. L.E.S., R.Z.H., G.W.M., T.G. and A.H. analyzed the data.

Funding

This work was supported by the National Institutes of Health (NIH) [HD 058070, ES 021985, NSF OCE1314480]; and a University of California, San Diego Academic Senate Grant [RN141S to A.H.]. L.E.S. was supported by a National Science Foundation Graduate Research Fellowship and a National Defense Science and Engineering Graduate Fellowship. Deposited in PMC for release after 12 months.

Supplementary information

Supplementary information available online at
http://dev.biologists.org/lookup/suppl/doi:10.1242/dev.126144/-/DC1

References

Ammerman, J. W. and Azam, F. (1982). Uptake of cyclic-amp by natural-populations of marine-bacteria. *Appl. Environ. Microbiol.* **43**, 869-876.

Aye, I. L. M. H., Paxton, J. W., Evseenko, D. A. and Keelan, J. A. (2007). Expression, localisation and activity of ATP binding cassette (ABC) family of drug transporters in human amnion membranes. *Placenta* **28**, 868-877.

Barnet, M. E. (2011). Dynamics of sea urchin gastrulation revealed by tracking cells of diverse lineage and regulatory state (Doctoral dissertation). California Institute of Technology. Pasadena, CA. 6146.

Belinsky, M. G., Bain, L. J., Balsara, B. B., Testa, J. R. and Kruh, G. D. (1998). Characterization of MOAT-C and MOAT-D, new members of the MRP/cMOAT subfamily of transporter proteins. *J. Natl. Cancer Inst.* **90**, 1735-1741.

Beltrán, C., Vacquier, V. D., Moy, G., Chen, Y., Buck, J., Levin, L. R. and Darszon, A. (2007). Particulate and soluble adenylyl cyclases participate in the sperm acrosome reaction. *Biochem. Biophys. Res. Commun.* **358**, 1128-1135.

Boadu, A. and Sager, A. (2004). Reconstitution of ATP-dependent cGMP transport into proteoliposomes by membrane proteins from human erythrocytes. *Scand. J. Clin. Lab. Invest.* **64**, 41-48.

Borst, P., de Wolf, C. and van de Wetering, K. (2007). Multidrug resistance-associated proteins 3, 4, and 5. *Pflugers Arch.* **453**, 661-673.

Bošnjak, I., Uhlinger, K. R., Heim, W., Smital, T., Franekić-Čolić, J., Coale, K., Epel, D. and Hamdoun, A. (2009). Multidrug efflux transporters limit accumulation of inorganic, but not organic, mercury in sea urchin embryos. *Environ. Sci. Technol.* **43**, 8374-8380.

Burke, R. D., Myers, R. L., Sexton, T. L. and Jackson, C. (1991). Cell movements during the initial phase of gastrulation in the sea urchin embryo. *Dev. Biol.* **146**, 542-557.

Burke, R. D., Lail, M. and Nakajima, Y. (1998). The apical lamina and its role in cell adhesion in sea urchin embryos. *Cell Adhes. Commun.* **5**, 97-108.

Chen, Z.-S. and Tiwari, A. K. (2011). Multidrug resistance proteins (MRPs/ABCCs) in cancer chemotherapy and genetic diseases. *FEBS J.* **278**, 3226-3245.

Chen, J.-H., Luo, Y.-J. and Su, Y.-H. (2011). The dynamic gene expression patterns of transcription factors constituting the sea urchin aboral ectoderm gene regulatory network. *Dev. Dyn.* **240**, 250-260.

Cole, S. P. C. (2014). Multidrug resistance protein 1 (MRP1, ABCC1), a "Multitasking" ATP-binding cassette (ABC) transporter. *J. Biol. Chem.* **289**, 30880-30888.

de Wolf, C. J. F., Yamaguchi, H., van der Heijden, I., Wielinga, P. R., Hundscheid, S. L., Ono, N., Scheffer, G. L., de Haas, M., Schuetz, J. D., Wijnholds, J. et al. (2007). cGMP transport by vesicles from human and mouse erythrocytes. *FEBS J.* **274**, 439-450.

Dormann, D. and Weijer, C. J. (2006). Chemotactic cell movement during Dictyostelium development and gastrulation. *Curr. Opin. Genet. Dev.* **16**, 367-373.

Fletcher, J. I., Haber, M., Henderson, M. J. and Norris, M. D. (2010). ABC transporters in cancer: more than just drug efflux pumps. *Nat. Rev. Cancer* **10**, 147-156.

Francko, D. A. (1989). Uptake, metabolism, and release of cAMP in selenastrum capricornutum (Chlorophyceae). *J. Phycol.* **25**, 300-304.

Fujino, Y. and Yasumasu, I. (1981). cAMP-dependent protein kinase in sea urchin embryos. *Gamete Res.* **4**, 395-406.

Gibson, A. W. and Burke, R. D. (1985). The origin of pigment cells in embryos of the sea urchin *Strongylocentrotus purpuratus*. *Dev. Biol.* **107**, 414-419.

Gibson, A. W. and Burke, R. D. (1987). Migratory and invasive behavior of pigment cells in normal and animalized sea urchin embryos. *Exp. Cell Res.* **173**, 546-557.

Godinho, R. O., Duarte, T. and Pacini, E. S. A. (2015). New perspectives in signaling mediated by receptors coupled to stimulatory G protein: the emerging significance of cAMP efflux and extracellular cAMP-adenosine pathway. *Front. Pharmacol.* **6**, 1-9.

Gökirmak, T., Campanale, J. P., Shipp, L. E., Moy, G. W., Tao, H. and Hamdoun, A. (2012). Localization and substrate selectivity of sea urchin multidrug (MDR) efflux transporters. *J. Biol. Chem.* **287**, 43876-43883.

Gökirmak, T., Shipp, L. E., Campanale, J. P., Nicklisch, S. C. T. and Hamdoun, A. (2014). Transport in technicolor: mapping ATP-binding cassette transporters in sea urchin embryos. *Mol. Reprod. Dev.* **81**, 778-793.

Goldstone, J. V., Hamdoun, A., Cole, B. J., Howard-Ashby, M., Nebert, D. W., Scally, M., Dean, M., Epel, D., Hahn, M. E. and Stegeman, J. J. (2006). The chemical defensome: environmental sensing and response genes in the *Strongylocentrotus purpuratus* genome. *Dev. Biol.* **300**, 366-384.

Griffiths, M. (1965). A study of the synthesis of naphthaquinone pigments by the larvae of two species of sea urchins and their reciprocal hybrids. *Dev. Biol.* **11**, 433-447.

Gross, J. M. and McClay, D. R. (2001). The role of Brachyury (T) during gastrulation movements in the sea urchin Lytechinus variegatus. *Dev. Biol.* **239**, 132-147.

Gustafson, T. and Wolpert, L. (1967). Cellular movement and contact in sea urchin morphogenesis. *Biol. Rev. Camb. Philos. Soc.* **42**, 442-498.

Hardin, J. (1989). Local shifts in position and polarized motility drive cell rearrangement during sea urchin gastrulation. *Dev. Biol.* **136**, 430-445.

Hardin, J. and McClay, D. R. (1990). Target recognition by the archenteron during sea urchin gastrulation. *Dev. Biol.* **142**, 86-102.

Henderson, M. J., Haber, M., Porro, A., Munoz, M. A., Iraci, N., Xue, C., Murray, J., Flemming, C. L., Smith, J., Fletcher, J. I. et al. (2011). ABCC multidrug transporters in childhood neuroblastoma: clinical and biological effects independent of cytotoxic drug efflux. *J. Natl. Cancer Inst.* **103**, 1236-1251.

Holland, N. D. and Jespersen, Å. (1973). The fine structure of the fertilization membrane of the feather star Comanthus japonica (Echinodermata: Crinoidea). *Tissue Cell* **5**, 209-214.

Hughes, J. N., Dodge, N., Rathjen, P. D. and Rathjen, J. (2009). A novel role for gamma-secretase in the formation of primitive streak-like intermediates from ES cells in culture. *Stem Cells* **27**, 2941-2951.

Jansen, R. S., Addie, R., Merkx, R., Fish, A., Mahakena, S., Bleijerveld, O. B., Altelaar, M., IJlst, L., Wanders, R. J., Borst, P. et al. (2015). N-lactoyl-amino acids are ubiquitous metabolites that originate from CNDP2-mediated reverse proteolysis of lactate and amino acids. *Proc. Natl. Acad. Sci. USA* **112**, 6601-6606.

Jedlitschky, G., Burchell, B. and Keppler, D. (2000). The multidrug resistance protein 5 functions as an ATP-dependent export pump for cyclic nucleotides. *J. Biol. Chem.* **275**, 30069-30074.

Jin, D., Ni, T. T., Sun, J., Wan, H., Amack, J. D., Yu, G., Fleming, J., Chiang, C., Li, W., Papierniak, A. et al. (2014). Prostaglandin signalling regulates ciliogenesis by modulating intraflagellar transport. *Nat. Cell Biol.* **16**, 841-851.

Kool, M., de Haas, M., Scheffer, G. L., Scheper, R. J., van Eijk, M. J., Juijn, J. A., Baas, F. and Borst, P. (1997). Analysis of expression of cMOAT (MRP2), MRP3, MRP4, and MRP5, homologues of the multidrug resistance-associated protein gene (MRP1), in human cancer cell lines. *Cancer Res.* **57**, 3537-3547.

Korolnek, T., Zhang, J., Beardsley, S., Scheffer, G. L. and Hamza, I. (2014). Control of metazoan heme homeostasis by a conserved multidrug resistance protein. *Cell Metab.* **19**, 1008-1019.

Leslie, E. M., Deeley, R. G. and Cole, S. P. C. (2001). Toxicological relevance of the multidrug resistance protein 1, MRP1 (ABCC1) and related transporters. *Toxicology* **167**, 3-23.

Litman, T., Druley, T. E., Stein, W. D. and Bates, S. E. (2001). From MDR to MXR: new understanding of multidrug resistance systems, their properties and clinical significance. *Cell. Mol. Life Sci.* **58**, 931-959.

Logan, C. Y. and McClay, D. R. (1997). The allocation of early blastomeres to the ectoderm and endoderm is variable in the sea urchin embryo. *Development* **124**, 2213-2223.

Manceau, S., Giraud, C., Declèves, X., Scherrmann, J. M., Artiguebieille, F., Goffinet, F., Chappuy, H., Vinot, C. and Tréluyer, J. M. (2012). ABC drug transporter and nuclear receptor expression in human cytotrophoblasts: Influence of spontaneous syncytialization and induction by glucocorticoids. *Placenta* **33**, 927-932.

Materna, S. C. and Davidson, E. H. (2012). A comprehensive analysis of Delta signaling in pre-gastrular sea urchin embryos. *Dev. Biol.* **364**, 77-87.

Materna, S. C., Ransick, A., Li, E. and Davidson, E. H. (2013). Diversification of oral and aboral mesodermal regulatory states in pregastrular sea urchin embryos. *Dev. Biol.* **375**, 92-104.

McAleer, M. A., Breen, M. A., White, N. L. and Matthews, N. (1999). pABC11 (also known as MOAT-C and MRP5), a member of the ABC family of proteins, has anion transporter activity but does not confer multidrug resistance when overexpressed in human embryonic kidney 293 cells. *J. Biol. Chem.* **274**, 23541-23548.

Medina, A. P., Lin, J. and Weigel, P. H. (2012). Hyaluronan synthase mediates dye translocation across liposomal membranes. *BMC Biochem.* **13**, 2.

Meyer Zu Schwabedissen, H. E. U., Grube, M., Heydrich, B., Linnemann, K., Fusch, C., Kroemer, H. K. and Jedlitschky, G. (2005). Expression, localization, and function of MRP5 (ABCC5), a transporter for cyclic nucleotides, in human placenta and cultured human trophoblasts: effects of gestational age and cellular differentiation. *Am. J. Pathol.* **166**, 39-48.

Miranda, E. R., Nam, E. A., Kuspa, A. and Shaulsky, G. (2015). The ABC transporter, AbcB3, mediates cAMP export in D. discoideum development. *Dev. Biol.* **397**, 203-211.

Müller, P. and Schier, A. F. (2011). Extracellular movement of signaling molecules. *Dev. Cell* **21**, 145-158.

Nigam, S. K. (2015). What do drug transporters really do? *Nat. Rev. Drug Discov.* **14**, 29-44.

Pratt, S., Shepard, R. L., Kandasamy, R. A., Johnston, P. A., Perry, W., III and Dantzig, A. H. (2005). The multidrug resistance protein 5 (ABCC5) confers resistance to 5-fluorouracil and transports its monophosphorylated metabolites. *Mol. Cancer Ther.* **4**, 855-863.

Ransick, A. and Davidson, E. (1998). Late specification of veg(1) lineages to endodermal fate in the sea urchin embryo. *Dev. Biol.* **195**, 38-48.

Ransick, A. and Davidson, E. H. (2006). cis-regulatory processing of Notch signaling input to the sea urchin glial cells missing gene during mesoderm specification. *Dev. Biol.* **297**, 587-602.

Rast, J., Cameron, R. A., Poustka, A. J. and Davidson, E. H. (2002). brachyury target genes in the early sea urchin embryo isolated by differential macroarray screening. *Dev. Biol.* **246**, 191-208.

Ravna, A. W., Sylte, I. and Sager, G. (2008). A molecular model of a putative substrate releasing conformation of multidrug resistance protein 5 (MRP5). *Eur. J. Med. Chem.* **43**, 2557-2567.

Reid, G., Wielinga, P., Zelcer, N., de Haas, M., van Deemter, L., Wijnholds, J., Balzarini, J. and Borst, P. (2003). Characterization of the transport of nucleoside analog drugs by the human multidrug resistance proteins MRP4 and MRP5. *Mol. Pharmacol.* **63**, 1094-1103.

Ricardo, S. and Lehmann, R. (2009). An ABC transporter controls export of a Drosophila germ cell attractant. *Science* **323**, 943-946.

Robert, H. S. and Friml, J. (2009). Auxin and other signals on the move in plants. *Nat. Chem. Biol.* **5**, 325-332.

Ruffins, S. W. and Ettensohn, C. A. (1996). A fate map of the vegetal plate of the sea urchin (Lytechinus variegatus) mesenchyme blastula. *Development* **122**, 253-263.

Sager, G. and Ravna, A. W. (2009). Cellular efflux of cAMP and cGMP - a question about selectivity. *Mini Rev. Med. Chem.* **9**, 1009-1013.

Sager, G., Ørvoll, E. Ø., Lysaa, R. A., Kufareva, I., Abagyan, R. and Ravna, A. W. (2012). Novel cGMP efflux inhibitors identified by virtual ligand screening (VLS) and confirmed by experimental studies. *J. Med. Chem.* **55**, 3049-3057.

Schulz, T., Schumacher, U. and Prehm, P. (2007). Hyaluronan export by the ABC transporter MRP5 and its modulation by intracellular cGMP. *J. Biol. Chem.* **282**, 20999-21004.

Development (2015) 142, 3537-3548 doi:10.1242/dev.126144

Sherwood, D. R. and McClay, D. R. (1999). LvNotch signaling mediates secondary mesenchyme specification in the sea urchin embryo. *Development* **126**, 1703-1713.

Shipp, L. E. and Hamdoun, A. (2012). ATP-binding cassette (ABC) transporter expression and localization in sea urchin development. *Dev. Dyn.* **241**, 1111-1124.

Smith, A. B., Pisani, D., Mackenzie-Dodds, J. A., Stockley, B., Webster, B. L. and Littlewood, D. T. J. (2006). Testing the molecular clock: molecular and paleontological estimates of divergence times in the Echinoidea (Echinodermata). *Mol. Biol. Evol.* **23**, 1832-1851.

Solek, C. M., Oliveri, P., Loza-Coll, M., Schrankel, C. S., Ho, E. C. H., Wang, G. and Rast, J. P. (2013). An ancient role for Gata-1/2/3 and Scl transcription factor homologs in the development of immunocytes. *Dev. Biol.* **382**, 280-292.

Soliman, S. (1984). Pharmacological control of ciliary activity in the young sea urchin larva: chemical studies on the role of cyclic nucleotides. *Comp. Biochem. Physiol. C Comp. Pharmacol.* **78**, 175-181.

Strouse, J. J., Ivnitski-Steele, I., Waller, A., Young, S. M., Perez, D., Evangelisti, A. M., Ursu, O., Bologa, C. G., Carter, M. B., Salas, V. M. et al. (2013). Fluorescent substrates for flow cytometric evaluation of efflux inhibition in ABCB1, ABCC1, and ABCG2 transporters. *Anal. Biochem.* **437**, 77-87.

Sweet, H. C., Gehring, M. and Ettensohn, C. A. (2002). LvDelta is a mesoderm-inducing signal in the sea urchin embryo and can endow blastomeres with organizer-like properties. *Development* **129**, 1945-1955.

Takata, H. and Kominami, T. (2004). Behavior of pigment cells closely correlates the manner of gastrulation in sea urchin embryos. *Zoolog. Sci.* **21**, 1025-1035.

Tresguerres, M., Levin, L. R. and Buck, J. (2011). Intracellular cAMP signaling by soluble adenylyl cyclase. *Kidney Int.* **79**, 1277-1288.

van de Ven, R., Scheffer, G. L., Reurs, A. W., Lindenberg, J. J., Oerlemans, R., Jansen, G., Gillet, J.-P., Glasgow, J. N., Pereboev, A., Curiel, D. T., et al. (2008). A role for multidrug resistance protein 4 (MRP4; ABCC4) in human dendritic cell migration. *Blood* **112**, 2353-2359.

Wei, Z., Angerer, R. C. and Angerer, L. M. (2006). A database of mRNA expression patterns for the sea urchin embryo. *Dev. Biol.* **300**, 476-484.

Whalen, K., Reitzel, A. M. and Hamdoun, A. (2012). Actin polymerization controls the activation of multidrug efflux at fertilization by translocation and fine-scale positioning of ABCB1 on microvilli. *Mol. Biol. Cell* **23**, 3663-3672.

Wielinga, P. R., van der Heijden, I., Reid, G., Beijnen, J. H., Wijnholds, J. and Borst, P. (2003). Characterization of the MRP4- and MRP5-mediated transport of cyclic nucleotides from intact cells. *J. Biol. Chem.* **278**, 17664-17671.

Wijnholds, J., Mol, C. A. A., van Deemter, L., de Haas, M., Scheffer, G. L., Baas, F., Beijnen, J. H., Scheper, R. J., Hatse, S., De Clercq, E. et al. (2000). Multidrug-resistance protein 5 is a multispecific organic anion transporter able to transport nucleotide analogs. *Proc. Natl. Acad. Sci. USA* **97**, 7476-7481.

Supplementary Methods:

Sp-C5a antibody generation and validation

Rabbit polyclonal antibodies to C5a (anti-C5a) were produced against recombinant C5a expressed in bacteria. The following N-terminal fragment of C5a was cloned into the pProEx Htb expression vector (Invitrogen) and expressed in BL21 Codon Plus cells: MIIEGNDPLSMTSPHRASEGDIHNDEGFGVQERSSSLEDQTVIEMDSQIDTALSYTDGK TPGELKDGRIGEQEDDPDETEQLLDKREEGDTEEQKSSNTGTKYWATGNFISVVTSQ WLTPLFRAAKKRGLNDDDLYHILPVDSAEKNAKIFAQLWEEEIKHHGGNAVKASLRRVI LR. Recombinant protein was produced and purified at the PEP Core facility of The Scripps Research Institute. Purified protein was run on polyacrylamide gels, and the protein bands were excised and sent to Lampire Biological Laboratories (Pipersville, PA) for antigen preparation, rabbit immunization, and affinity purification. The recombinant protein was used to affinity-purify an aliquot of the C5a-specific IgG from antiserum. This affinity-purified antibody was used for Western blots, while adsorbed whole serum (described below) was used for immunohistochemistry (IHC) (and affinity-purified antibody was tested with IHC as a control).

To determine specificity of anti-C5a, we used Western blots to compare protein expression between embryos expressing endogenous C5a, overexpressing C5a-mCherry, and expressing no C5a (i.e. MASO knockdown) (Fig. S1A). Western blotting was performed with 70 hpf embryos from the same batch, and samples included: (1) C5a-CmCherry overexpressing (0.8 mg/ml), (2) control-injected (0.05 mg/ml histone H2B-CFP), (3) control-uninjected, (4) C5a knockdown with MASO1 (300 µM), and (5)

C5a knockdown with MASO2 (600 µM). Ten embryos were pooled for the C5a-CmCherry over-expressing lane, and 200 embryos were pooled per lane for the control-injected, control-uninjected, MASO1, and MASO2 samples.

Antibody adsorption for immunohistochemistry: Because an 80 kDa band inconsistent with mature C5a appeared strongly on blots of all developmental stages, while the 210 kDa C5a band appeared only after 26 hpf, anti-C5a whole serum was adsorbed to fixed and permeabilized 22 hpf embryos to remove immunoglobulins reacting with non-C5a antigens. Sera (diluted to 1:1500 in 2% BSA-PBS) were adsorbed for 24 hours at 15°C and then collected and stored at 4°C with 5 mM sodium azide prior to immunolocalizion of C5a. Examples of C5a immunolocalizations are shown using pre- and post-adsorbed antibody (Fig. S1B,C). After adsorption, localization was restricted to *gcm*-expressing pigment cells, consistent with the localization of *C5a* transcripts (Fig. 3).

Time-lapse imaging of C5a-knockdown embryos

Embryos were mounted in FSW on protamine sulfate-coated Delta-T dishes (Bioptechs, Butler, PA) and retained in an enclosure of Scotch double-sided tape, with four ~50 µm channels through which FSW could flow (Fig. S3). A coverslip was placed on top of the tape to restrict embryo movement. A chilled stage maintained embryos at 15°C, and images were captured on a Leica Sp8 confocal microscope with a Plan-Apochromat 20X objective (0.7 numerical aperture). In long time-lapses (> 15 hours), embryonic development was slowed to ~0.5-0.75 times the normal rate.

Supplemental Figures:

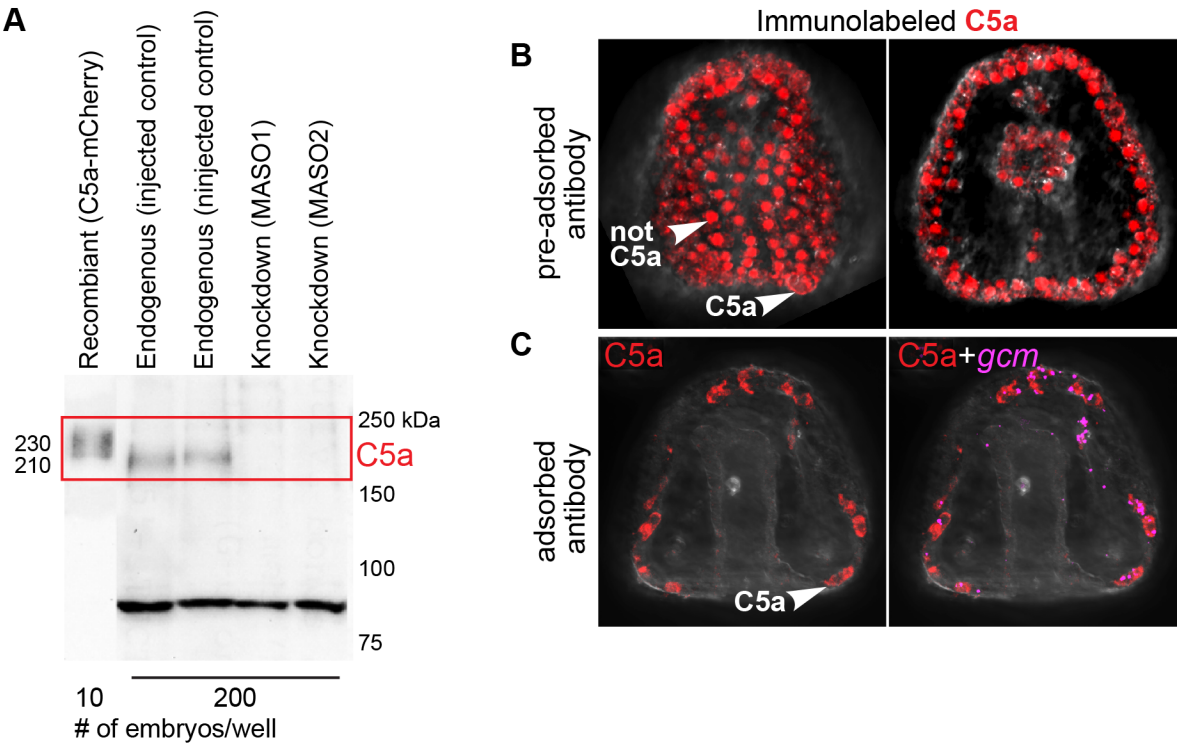

Figure S1. Detecting C5a with affinity-purified and adsorbed anti-C5a, and demonstrating knockdown with two MASOs.

(A) Western blot using lysates from 70 hpf embryos, probed with affinity-purified anti-C5a. C5a-mCherry runs as a ~230 kDa doublet, while endogenous C5a runs at 210 kDa. Ten embryos were lysed and run per lane for the C5a-mCherry sample, while 200 embryos per lane were run for all other samples. Endogenous C5a (210 kDa band) is knocked down by both C5a MASO1 and MASO2, while an ~80 kDa band not corresponding to C5a is unaffected by both MASOs. Lysate from the ten C5a-mCherry overexpressing embryos had insufficient ~80 kDa antigen to be detected in the first lane.

(B,C) Immunolocalization of C5a (red) in prism stage embryos using pre- and post-adsorbed anti-C5a (from whole serum).

(B) Embryo is immunolabeled with pre-adsorbed anti-C5a serum. Two z-sections are shown. Pre-adsorbed anti-C5a recognizes a nuclear antigen (likely corresponding to the 80 kDa band seen in (A)) in most cells. In addition, in only cells with pigment cell-like distribution around the embryo, it recognizes a membrane-localized and intracellular signal corresponding to C5a.

(C) Embryo is immunolabeled with adsorbed anti-C5a serum, and *gcm* transcripts (magenta) are labeled with FISH. Adsorbed anti-C5a does not detect a nuclear antigen, but recognizes membrane-localized and intracellular C5a in *gcm*-expressing pigment cells, which is consistent with the localization of *C5a* transcripts in *gcm*-expressing cells (Fig. 3).

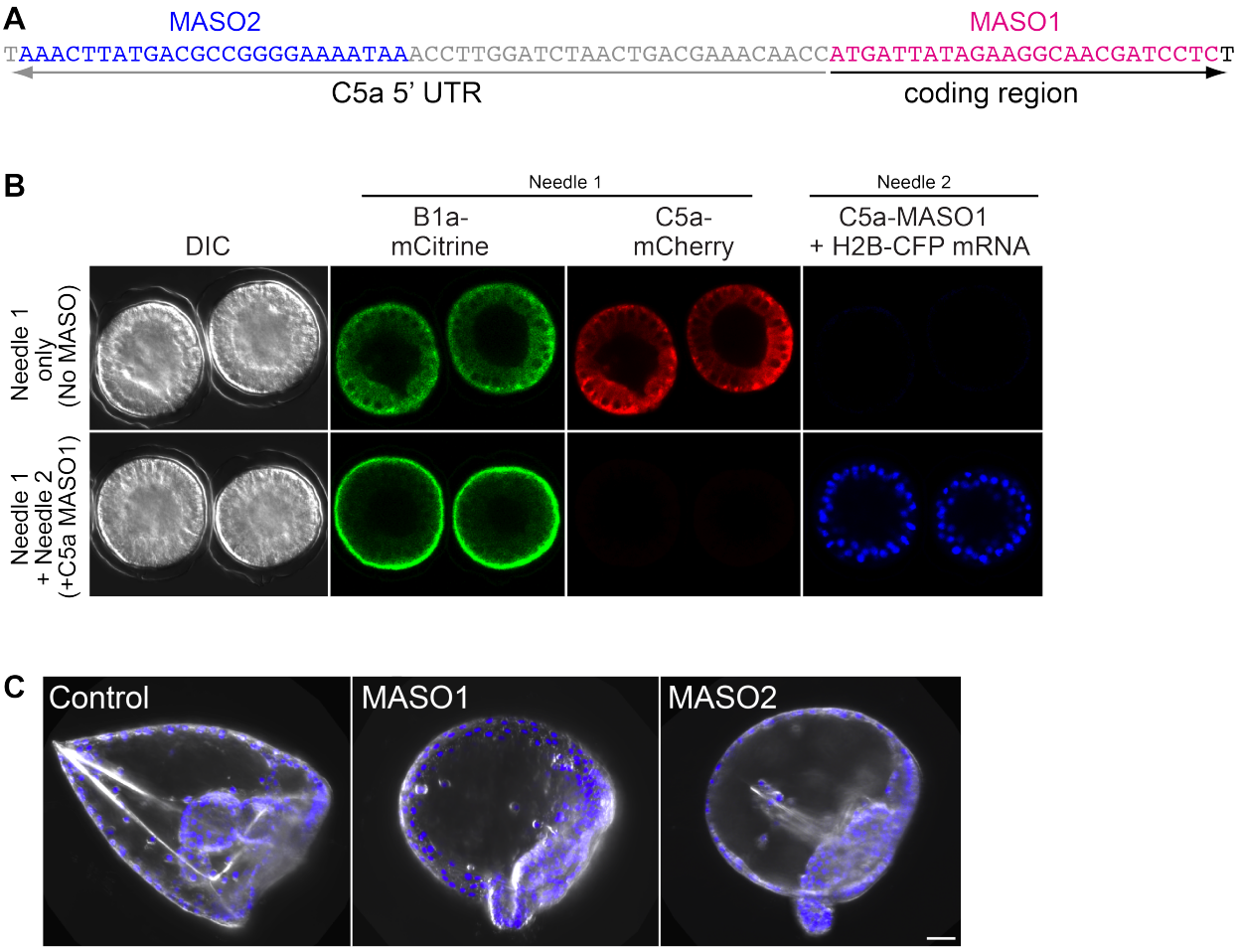

Figure S2. Two MASOs block translation of *C5a* and cause hindgut prolapse.

(A) Two non-overlapping MASOs block translation of *C5a*. MASO1 targets the first 25 bases of the coding region, while MASO2 targets the 5' UTR.

(B) C5a-MASO1 knocks down C5a-mCherry, but not B1a-mCitrine. Fertilized eggs were all injected with Needle 1, containing 1 mg/ml each of B1a-mCitrine and C5a-mCherry mRNA and imaged at the 20 hpf blastula stage. In the top panel (no MASO), both B1a-mCitrine and C5a-mCherry are expressed.

In the bottom panel, samples were injected a second time with Needle 2, containing 0.3 mM C5a-MASO1 and H2B-CFP mRNA as an injection marker. In the presence of MASO1, no C5a-mCherry expression is detected, while B1a-mCitrine is robustly

expressed. B1a-mCitrine localizes to apical membranes, presumably due to a relief on the protein sorting machinery, as C5a-mCherry is no longer present as a membrane-bound protein.

Interestingly, in the absence of MASO, neither protein membrane-localizes, presumably because the trafficking machinery is overwhelmed. Consistent with this hypothesis, B1a trafficking is normal in the presence of C5a-MASO1.

(C) Both MASO1 and MASO2 cause hindgut prolapse as shown in 70 hpf embryos. The phenotypes that result from injection of MASO1 and MASO2 are indistinguishable. Nuclei (blue) are labeled with H2B-CFP. Scale bar is 20 μm.

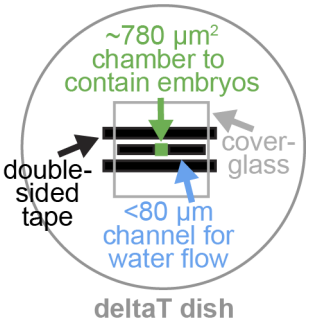

Figure S3. Chambers used to contain swimming embryos for long-term imaging.

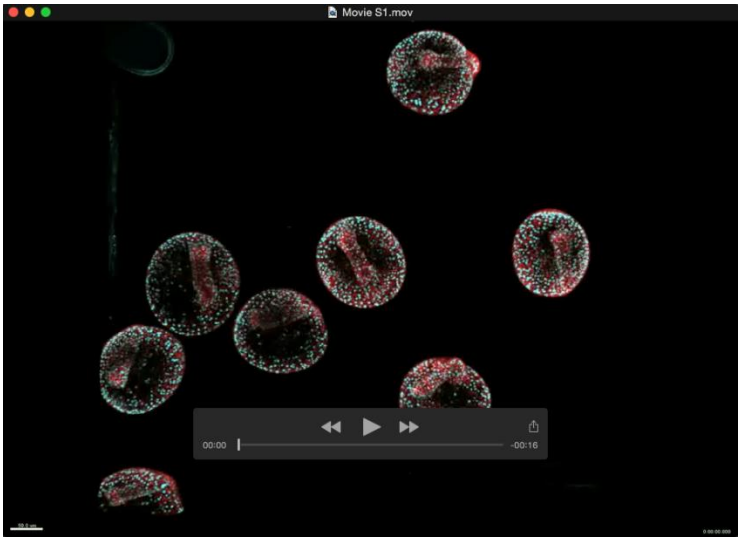

Movie 1: Maximum intensity projection (MIP) time-lapse of seven C5a knockdown embryos. Plasma membranes are red (LCK-mCherry), and nuclei are blue (H2B-CFP). 46 hpf embryos were imaged every 10 minutes for 144 frames (~24 h). The video is sped up 5355X. Scale bar (bottom left) is 50 µm.

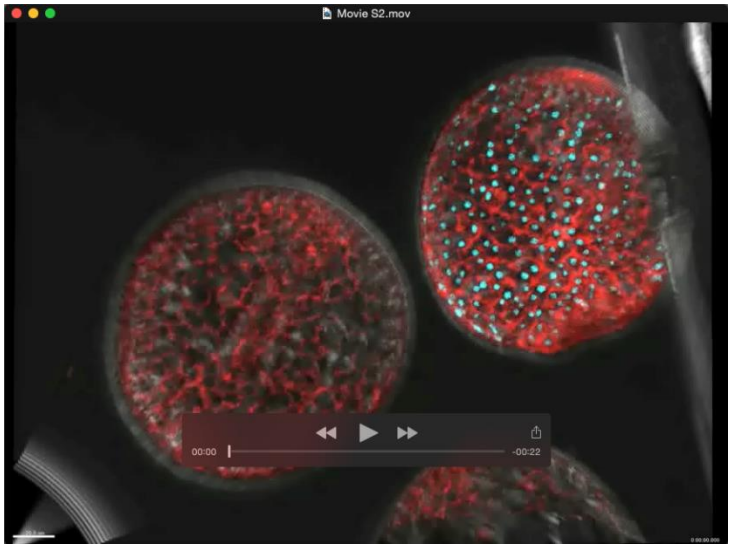

Movie 2: MIP (fluorescent channels plus brightfield) time-lapse of a control embryo (left, red membrane) and a C5a knockdown embryo (right, red membrane and blue nuclei) shown side by side. 48 hpf embryos were imaged every 2.5 min for 432 frames (~18 h). The video is sped up 3085X. Scale bar (bottom left) is 20 µm.

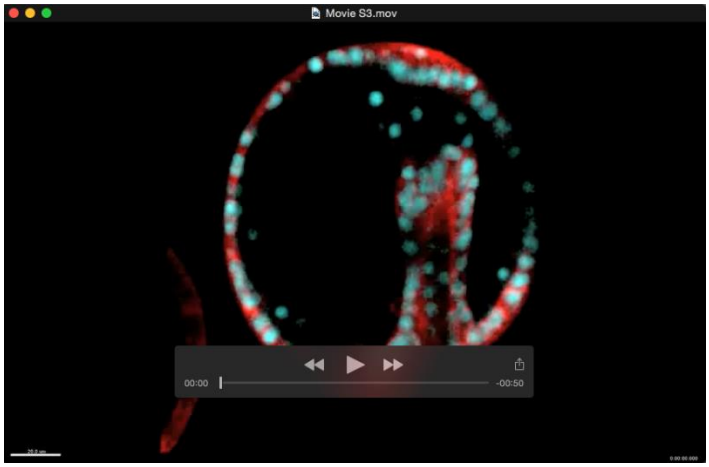

Movie 3: Cross-section of the C5a knockdown embryo from Movie 2, shown as a partial MIP with raw fluorescence, then repeated with isosurface renderings. Scale bar (bottom left) is 20 μm.